Trends in Developmental Biology
Vol. 6, 2012

Review

Calcium transients and gene expression during the MBT stage of Xenopus

Verónica Narváez-Padilla[1] and José Díaz[2,*]

[1]Developmental Biology Laboratory, [2]Theoretical and Computational Biology Group, Facultad de Ciencias, Universidad Autónoma del Estado de Morelos, Av. Universidad 1001, Colonia Chamilpa, Cuernavaca, Morelos, C.P. 60209, México

ABSTRACT

During the Mid Blastula Transition Stage (MBT) a series of calcium transients arise at a narrow zone of the presumptive dorsal ectoderm. These transients establish a long-distance permissive signal that coordinates the spatio-temporal events that lead to the ventralization of the embryo. However, given the fact that these transients are generated at the dorsal side of the MBT blastula, it is of interest to understand how they can induce ventral features in the blastomeres that are located at the opposite side of the calcium source. In order to propose a plausible hypothesis to answer this question, this review is not only an exhaustive revision of the literature about calcium and the MBT in Xenopus, but tries to integrate this knowledge into a dynamical vision of the role of calcium in the ventralization of the blastula. In this dynamical scenario, the frequency of the calcium signal can have a central role in the control of the activation of the genes that impel the expression of the dorsal and ventral features of the blastula. In this form, calcium could exert a dual regulation of the inductive signals that patterns the midblastula. However, the scarce experimental and theoretical literature about the generation and role of calcium in the mid blastula transition makes this objective hard to be reached. However, this work tries to identify the main unsolved problems in this field and propose a series of hypothesis that can promote further experimental and theoretical research.

KEYWORDS: calcium transients, gene expression, Xenopus mid blastula transition

*Corresponding author
biofisica@yahoo.com

1. INTRODUCTION

1.1. Xenopus early development and mid blastula transition

Xenopus development begins when the spermatozoon enters the ovule cytoplasm. Fertilization (Figure 1) produces a 30^{o} rotation of the cortical cortex of the egg, producing a rearrangement of the maternal components of the cytoplasm [1], which defines the dorso-ventral and antero-posterior axes. The cytoplasm opposite to the sperm entry point, known as the Nieuwkoop Center (NwC), contains dorsal determinants, which will induce the primary organizer (Spemann Organizer). The organizer is able to induce gastrulation and defines the pattern of axial structures.

Xenopus egg has two well-defined cytoplasmic regions (Figure 2a): 1) the animal pole, in which the nucleus is located after fertilization and 2) the vegetal pole, in which most of the yolk is stored. The first mitotic furrow (Figure 1) surges from the point of entry of the sperm and goes through the NwC, splitting it in two halves. In this form, the plane of bilateral symmetry of the embryo is defined [2]. This first cell cycle takes approximately 90 minutes but the next eleven are quick (20-30 minutes), synchronized cell divisions, with

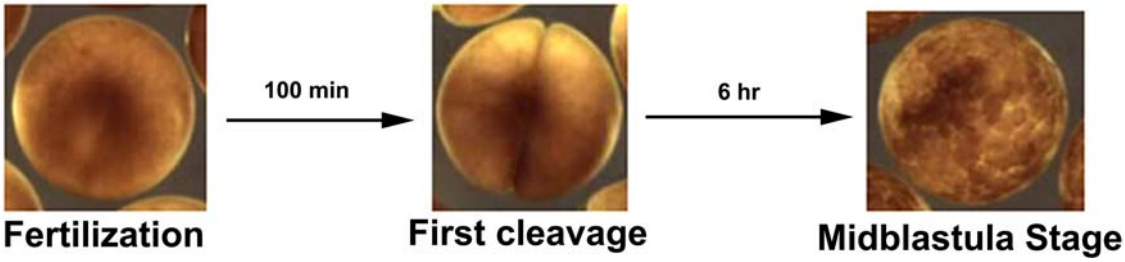

Figure 1. The first cleavage of the Xenopus egg occurs 100 min post-fertilization. The embryo reaches the MBT stage after the 12th cell division, about 6 hrs after fertilization.

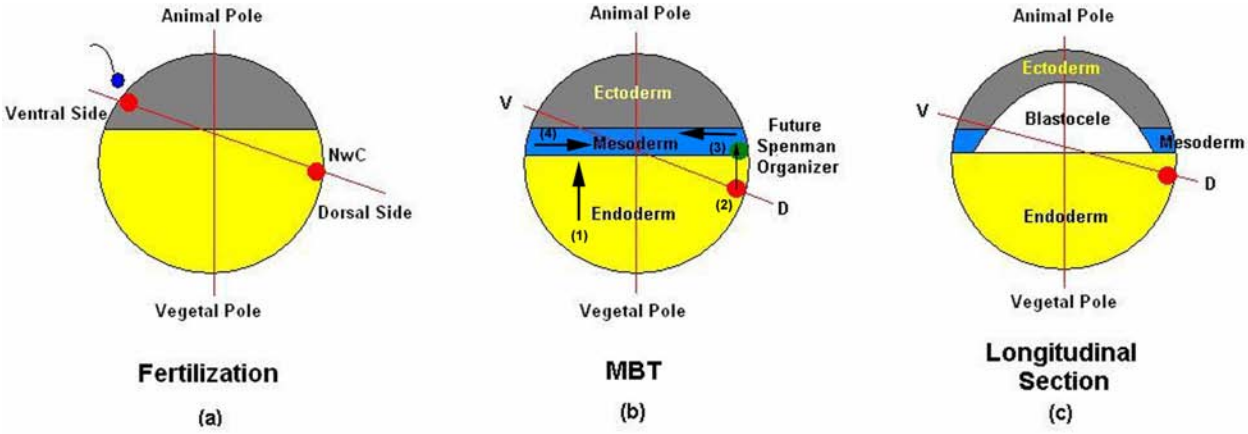

Figure 2

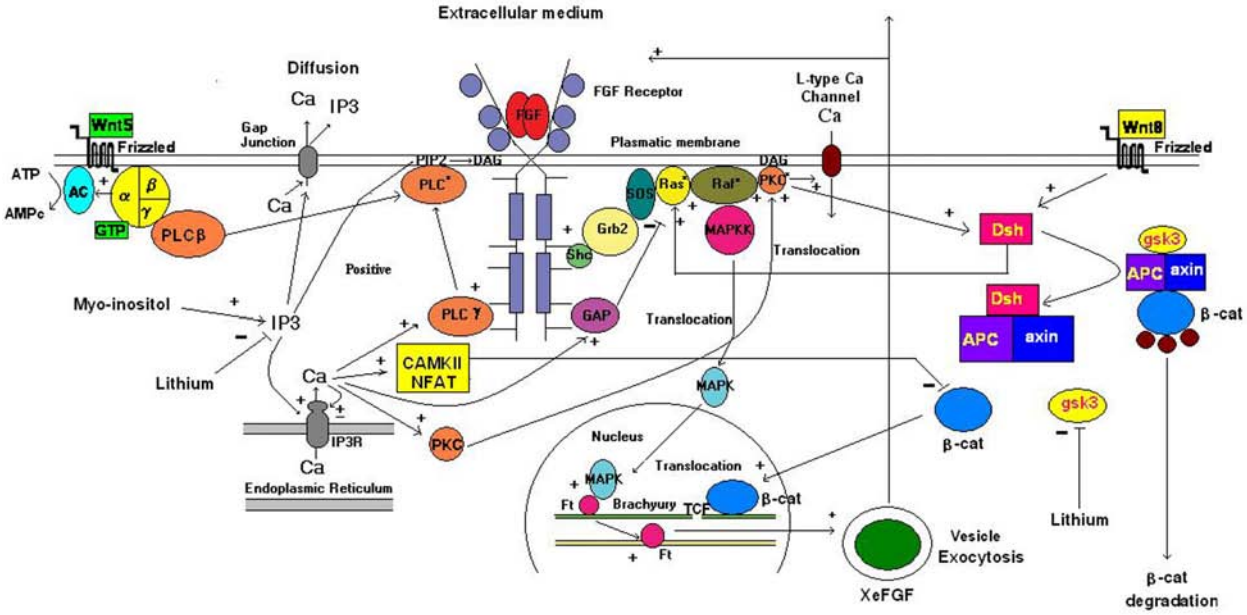

Figure 3

no gap phases. By that time the embryo is a smooth, spherical ball of approximately 4000 cells. It has a cavity filled with fluid (blastocoel) where three regions can be defined: the animal cap, which is the roof of the blastocoel, and gives rise to the ectoderm; the vegetal mass (the blastocoel floor), which becomes endoderm, and the marginal zone (the walls of the blastocoel) which are induced to becomes mesoderm (Figure 2b). At the 13th division, the synchrony is lost, as the gap phases appear and the zygotic genetic machinery is turned on by early transcription factors of maternal origin [3]. This stage is known as the mid blastula transition (MBT). Gastrulation begins at the 15th cycle, with the appearance of the dorsal blastopore lip (the organizer). At this stage mitosis stops. The movements during gastrulation conclude with the formation of the three germ layers and the establishment of the definitive antero-posterior and dorso-ventral axes [4].

With the cortical rotation that occurs after fertilization, cytoplasmic dorsal determinants are translocated to the future dorsal side. Therefore there is an asymmetrical activation of the Wnt/ β-catenin signaling pathway and accumulation of more β-catenin in dorsal nuclei. β-catenin is required to transcriptionally activate dorsal-specific genes at the mid blastula transition (MBT).

1.2. Patterning of the early embryo

The induction, specification, formation and differentiation of the mesoderm is a dynamical process in which four convergent signaling pathways interact (Figure 2b): The first pathway, triggers a general mesodermal inducing signal that is produced by all vegetal cells which induce adjacent marginal cells to become mesoderm. This pathway depends on the maternal transcription factor VegT, as was shown by Kofron and collaborators [5]. Depletion of VegT resulted in the loss of almost all of mesodermal tissue. They found no expression of mesodermal markers such as MyoD, cardiac actin, Xbra, Xwnt8 and alphaT4 globin. Also, they showed that eFGF, FGF3, FGF8, and the TGFbs, Xnr1, Xnr2, Xnr4 and *derrière* were directly or indirectly activated by VegT, and that these zygotic growth factors are responsible for the induction of the mesoderm. Previously it was demonstrated that the FGF signalling pathway is required to maintain the expression of XBra [6], and in *Xenopus*, disruption of FGF signaling inhibits the transcription-inducing activity of VegT and Xbra expression, even at the doses where VegT is known to robustly induce Xbra expression [4, 7, 8], therefore it seems that a regulatory loop is established where XBra activates a member of the FGF family and FGF

Legend to Figure 2. (a) During fertilization the Dorso-Ventral (D-V) axis is defined between the site of entrance of the embryo and the Nieuwkoop Center (NwC), which is settled down just at the opposite side. The Animal and Vegetal poles define the Animal-Vegetal (A-V) axis. (b) At Mid blastula Transition (MBT) the blastula is divided into three prospective regions: the ectoderm at the animal pole; the endoderm at the vegetal pole and the mesoderm in the marginal zone of the embryo. The patterning of the mesoderm is due to four signals that converge in the equatorial zone of the blastula: (1) ventralizing signal from the vegetal pole along the A-V axis; (2) dorsalizing signal from the NwC that defines the Spemann organizer; (3) dorsalizing signal from the prospective Spemann organizer and (4) ventralizing signal from the ventral side of the embryo. (c) Longitudinal section of the MBT blastula showing the relative position of the germinal layers with respect to the blastocoel or internal fluid-filled cavity of the embryo.

Legend to Figure 3. Interaction of the Wn5/Ca^{2+}, FGF/MAPK/Ca^{2+} and Wnt8/β-Catenin at the MBT stage of Xenopus embryo. Both FGF and Wnt5 turn on the IP_3-Ca^{2+} second messenger system, which together with gsk3, allow the expression of the ventral features of the embryo. Ca^{2+} activates both CAMKII and NFAT that inhibit the dorsalizing action of β-Catenin. Activation of the IP_3-Ca^{2+} system also turns on PKC, which in turn activates Dishevelled (Dsh), increasing the expression of the MAPK at the Ras level. Furthermore, PKC directly increases the expression of the MAPK by enhancing the action of Raf on the kinases downstream. The IP_3-Ca^{2+} system also modulates MAPK cascade activity by enhancing the inhibitory action of the GAP protein on Ras. Lithium blocks either gsk3 or the PI cycle (at the level of the enzymes such as inositol-1-phosphatase, and inositol monophosphatase), allowing the expression of the dorsal features induced by Wnt8 through the activation of β-Catenin. MAPK induces the activation of Xenopus *Brachyury*, which is a marker of mesoderm formation.

maintains expression of mesodermal genes, such as XBra [9].

The second pathway is a dorsalizing signal from the Nieuwkoop center. The Nieuwkoop center is localized in vegetal cells at the marginal zone. It was defined as cells that were able to produce signals that induce dorsal mesoderm (notochord and muscle), as opposed to the rest of the vegetal cells that induce ventral mesoderm (blood and mesenchyme), while retaining an endodermal fate. The Nieuwkoop center is required to induce the overlaying animal cells at the marginal zone to become the organizer. Cortical rotation triggered after fertilization translocated to the future dorsal marginal region components of the Wnt pathway that were maternally deposited in the vegetal region. These components include Wnt11 mRNA, Dishevelled (Dsh) and GSK3-binding protein (GBP). When Wnt11 protein binds to its receptor Frizzled (Xfz7) the Wnt 8/β-Catenin pathway or canonical Wnt pathway is activated in the Nieuwkoop center. This results in the inhibition of a complex composed of Axin/Conductin, the adenomatous polyposis tumor suppressor protein (APC), Diversin and GSK-3 which phosphorylates β-catenin protein targeting it for degradation via the ubiquitine-proteosome system [10, 11]. To inactivate this complex, Dsh interacts with Axin and recruits GBP, displacing GSK3 from the destruction complex. Therefore, β-catenin is stabilized and accumulates during MBT at the dorsal marginal zone of the embryo [12] (Figure 2b). β-catenin interacts with the transcription factor LEF/TCF allowing the expression of dorsal features of the mesoderm [13].

The third signal emanates from the organizer and defines dorsal structures. It was shown that FGF signaling is required for the formation of dorsal (notochord) and paraxial (axial skeleton, skeletal muscles and dermis), while inhibiting ventral mesoderm, such as blood formation [14, 15]. It is thought that FGF signalling promotes dorsal fates by inhibiting the expression and activity of BMPs, which promote ventral fates. It has been shown that the expression of BMP antagonists chordin and noggin is dependant of FGF signalling. Also, FGF signalling has been shown to inhibit BMP signalling via ERK-dependent phosphorylation of the linker domain of Smad1, a crucial intracellular mediator of BMP signalling [16].

The fourth signal comes from the ventral region, defining ventral structures of the mesoderm [2, 3]. This ventralizing signal along the prospective mesoderm is probably due to the synergetic interaction of BMPs, the FGF/Ca^{2+} and Wnt5/Ca^{2+} (noncanonical Wnt) signaling pathways. In *Xenopus*, it was shown that CaMKII is activated by Wnt and Frizzled (Fz) receptors promoting ventral cell fates [17]. On the other hand, the inhibition of BMP-4 signaling abolishes ventral mesoderm formation, however, inhibition of FGF signaling converts dorsal to ventral mesoderm so it is suggested that inhibition of FGF signaling ventralizes the mesoderm, at least in part, via BMP activation [18]. The interaction between the FGF/Ca and Wnt5/Ca pathway is discussed below.

2. Ca^{2+} dynamics in Xenopus blastula at MBT

An intriguiting fact during Xenopus development is the appearance at the **MBT** stage of a zone of intense periodic calcium signaling, located at the anterior dorsal part of the animal side (prospective ectoderm) of the embryo. Leclerc and collaborators [19] recorded these calcium transients using a Photon Imaging Microscope after injection of the calcium-sensitive bioluminiscent reporter f-aequorin into the dorsal micromeres of 8-cell stage embryos (Figure 4a). The number of calcium transients varies from 2 to 6 at the MBT (stage 8, around 4-5 hours pf) and increases to ~84 at stage 11 (around 12 hours pf) At the MBT, the duration of the calcium transients was of ~38 s, with an average period of 750 s [19]. In Figure 4b is shown the spatial distribution of these calcium transients.

The onset of this calcium signaling source represents a challenge for the undestanding of the molecular processes that underlay the spatio-temporal dynamics of specification of the ventral characteritics of the prospective mesoderm of the Xenopus embryo.

According to Kume and collaborators [20, 21], injection of lithium at the 8-cells stage induces the dorsalization of the embryo and reduction of posterior structures, and the normal phenotype is rescued by injection of myo-inositol (an intermediate of the phosphatydilinositol (PI) cycle). In Figure 3 it is shown the possible targets of lithium. Both gsk3 and the PI cycle can be blocked by lithium, indicating that the IP_3-Ca^{2+} signaling system together

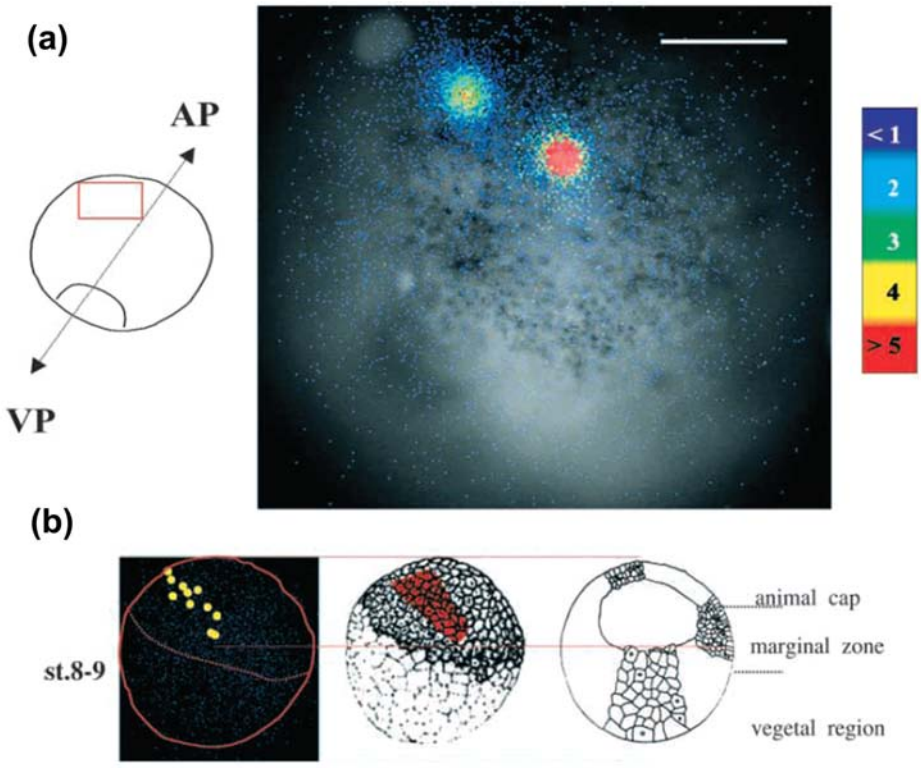

Figure 4. (a) Calcium transients registered at the prospective dorsal ectoderm of the Xenopus embryo at stage 10.5. The color bar shows the intensity of the signal. Color red represents the maximum intensity of the signal; (b) Localization of the calcium transients in a narrow region of the prospective dorsal ectoderm of Xenopus from stage 8 to 9. [Reproduced with permission from Leclerc, C., Webb, S. E., Daguzan, C., Moreau, M. and Miller, A. L. 2000, Journal of Cell Science, 113, 3519].

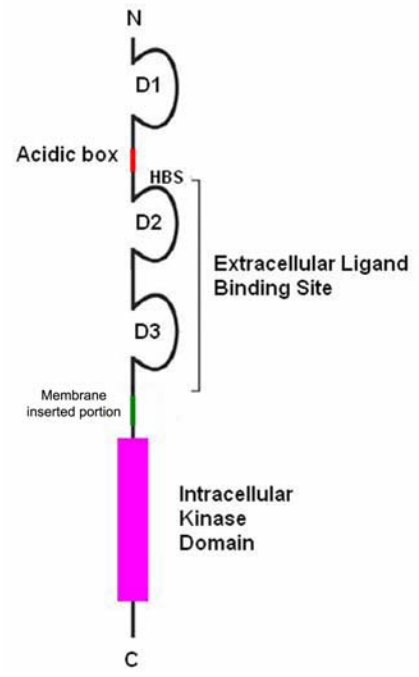

Figure 5. Structure of the FGF receptor. Its immunoglobulins-like extracellular portion is composed by three loops or domains marked as D1, D2 and D3. Between D1 and D2 is the acidic box (red color), which is an exclusive feature of this kind of receptors. D2 and D3 form the ligand binding portion of the receptor. The kinase domain of the receptor is located in its intracellular portion (magenta color). In the D2 loop there is an amino acid sequence that forms the heparin binding site (HBS). The FGF receptor is inserted in the membrane by its amino acid sequence located between D3 and the kinase domain (green color).

with gsk3 has influence in the determination of the ventral features of the embryo. Additional experimental results supporting this hypothesis were obtained by injecting monoclonal antibodies that block the IP_3 receptor (IP3R) at the endoplasmic reticulum of ventral blastomeres. The effects of the blocking of the IP3R results in the supression of the IP3 induced-Ca^{2+} release (IICR), induces dorsal development and gives rise to body axis duplication [20, 21]. The spatial expression pattern of the IP3R during early development of Xenopus was determined by inmunohistochemistry [20]. It was found that the IP3R is uniformily distributed along the D-V axis, which is in accordance with the previous results obtained in [22] where the ectopically expressed PI-coupled 5-hydroxytryptamina receptor produces equivalen Ca^{2+} signals in both ventral and dorsal halves of the Xenopus embryo.

These results make clear that the ventralization of the Xenopus embryo depends not only on the presence of the maternal molecule gsk3 but also on the IP_3-Ca^{2+} dynamics. However, these results are also paradoxical: the even distribution of the IP3R along the D-V axis aparentely contradicts the experimental results reported in [19] because: 1) the source of the calcium spikes is restricted to a narrow zone of the ectoderm, and 2) the calcium transients are generated at the dorsal side of the embryo, not at the ventral one.

These two intriguing facts should be clarified by using two approaches: 1) the molecular biology approach, in order to identify the key molecular events that generate the calcium signal that acts like a ventralizing signal; 2) the systems biology approach, which uses mathematical and computational tools to characterize the spatio-temporal dynamics of the calcium-depending ventralizing process.

3. FGF/Ca^{2+} signaling pathway

3.1. Molecular biology of the FGF signaling pathway

There are three subgroups of the Fibroblast Growth Factor (FGF) family: the canonical FGFs, the intracellular FGFs and the hormonal FGFs. The canonical FGF represents a family that comprises about 20 isoforms; they exert their action by short range diffusion in the extracellular medium, and can act in a dose-dependent fashion [23].

Canonical FGFs are secreted ligands that bind to their specific cell surface receptor belonging to a tyrosine kinase family, the FGF receptors (FGFR). In vertebrates, there are four genes (*FGFR1-4*), and FGFs bind to these receptors with different affinity (k_d) values that ranges from about 6.19 x 10^{-8} M to 1.65 x 10^{-7} M [24, 25]. The four FGFR isoforms are very similar in their global structure with an extracellular-ligand-binding domain, a single transmembrane domain and an intercellular tyrosine kinase domain. The extracellular portion of the receptor has two or three immunoglobulin (Ig)-like domains and a heparin-binding domain which is important for the interaction with the ligand. This extracellular domain suffers multiple alternative splicing, which modulates the affinity of the receptor to its ligand. Between the extracellular domains D1 and D2 (Figure 5) there is a consecutive file of acidic amino acids building up the acidic box, which is an exclusive feature of these receptors [23, 24]. The acidic box is connected to the ligand binding portion of the receptor, which consists of two loops formed by domains D2 and D3. The heparin-binding site is located in de D2 loop. The tyrosine kinase domain of the receptor is located in the cytoplasm.

Once FGF binds to its receptor, two ligand-receptor complexes forms a dimeric complex $(FGF\text{-}FGFR)_2$ by mutual phosphorylation. This triggers the activation of signal transduction pathways such as Ras-MAPK, the Akt, or the PKC pathways [25, 26, 27].

The subgroup of intracellular FGFs (iFGFs) or FGF Homologous Factor (FHFs) share a common structural core with the other FGFs, but are not secreted and are unable to bind FGFR. They contain a nuclear localization signal [28]. Members of this subgroup are *fgf11, fgf12, fgf13* and *fgf14*. They seem to be involved in neuronal function [29].

The hormone-like FGFs (hFGFs) act as endocrine factors. They have a reduced affinity to heparin sulfate and require the presence of Klotho, a transmembrane protein, to be able to bind the FGFR. hFGFs are specific of vertebrates. Their major role has been found in metabolism at

postnatal stages, but they seem to participate as well during embryonic development.

This work will focus only on canonical FGFs pathways in Xenopus early development. In Xenopus embryos, the most abundant FGFs at the beginning of the MBT are: basic FGF (bFGF), which is also known as isoform FGF2 and the Xenopus embryonic FGF (XeFGF), which is related to the isoform FGF4. These are proteins of ~ 16 to 26 kDa, of maternal origin, and apparently distributed all over the Xenopus embryo [25, 30]. FGFR is located all over the embryo but enhanced at the marginal zone of the embryo [25, 30]. Upon the binding of FGF to its receptor, a dimeric complex is formed, triggering the phosphorylation of specific intracellular tyrosine residues: Y456, Y583, Y585, Y653, Y654, Y730 and Y766 to which a series of specific proteins are attached.

Figure 3 shows that in the Xenopus blastomere the dimeric complex $(FGF\text{-}FGFR)_2$ phosphorylates three specific proteins. These proteins are: the docking Sh2-Sh3 adaptor protein Shc, which binds to the phosphorylation sites Y653 and Y654; Phospholipase C (PLC), which binds to the phosphorylation site Y766 and a GTP-ase Activating Protein (GAP), which probably binds to the phosphorylation sites Y653 or Y654 [31, 32]. After the cross-phosphorylation of the FGF-FGFR complexes, the chemical signal generated by the external FGF concentration is transmitted to the small G-protein Ras through the docking proteins Shc, Grb2 and SOS (Figure 3). The activated state of Ras is regulated by GAP, which is activated by the dimeric form of the FGF receptor. Once Ras is activated, the signal is transmitted downstream through a MAPK cascade in which the MAPKKK (MAP-Kinase-Kinase-Kinase) is Raf1. This serine/threonine kinase is translocated to the inner side of the cell membrane and activated by Ras, in presence of phosphatidic acid. Activated Raf specifically phosphorylates either MEK1 or MEK2, which is a MAPKK (MAP-Kinase-Kinase) that phosphorylate tyrosine and threonine residues of a MAPK (MAP-Kinase). In *Xenopus*, this MAPK can be either ERK1 or ERK2 and a fraction of it is translocated into the nucleus and activates genes such as Xbra. Xbra expression is enhanced at the marginal zone of the blastula, principally at the dorsal side, under the action of FGF [7, 27, 33, 34, 35, 36].

The Xbra gene has a regulatory palindromic sequence in its promoter, to which the dimeric form of the Xbra transcription factor binds. In contrast, the gene XeFGF (FGF of Xenopus) has a regulatory region that is a half of the palindromic sequence of the Xbra gene and is located at the position -923 from the transcription starting site. The monomeric form of the Xbra transcription factor binds to this site activating the transcription of the gene XeFGF. In Figure 3 it is shown that the co-activation of XeFGF closes a positive feedback loop, in which the binding of FGF to its receptor induces the production of embryonic FGF.

This sequence of chemical steps forms the basic process of mesoderm induction and regulation by FGF. However, the binding of FGF to its receptor also contributes to the activation of the IP_3-Ca^{2+} signaling pathway that can spatially and temporally modify the signal transmitted by the MAPK cascade.

3.2. Activation of the IP_3-Ca^{2+} signaling pathway by FGF

Cells of all organisms are subjected to an asymmetric distribution of ions between their extracellular and intracellular environment. In the case of the calcium ion (Ca^{2+}), the external concentration can be as high as 1 mM, while the intracellular concentration is about ~100 nM in most of the cells [37]. The lumen of the endoplasmic reticulum (ER) has a set of proteins like the calsequestrin, which are able of fixing Ca^{2+} allowig concentrations up to 1 mM [37]. In consequence, the high Ca^{2+} concentration in the ER lumen and in the extracellular medium set up an intense electrochemical gradient that drives the flow of this ion into the cytoplasm. However, high concentrations of intracellular Ca^{2+} are toxic for the cell. In consequence, there is a series of mechanisms that regulate its basal concentration. The ATPases of the cell and ER membranes counteract the calcium flow by pumping this ion back to the ER lumen or pumping it out of the cell. Other homeostatic mechanisms are the Na^{+}-Ca^{2+} exchangers of the cell membrane and the calcium excahngers of the mitochondrial membrane. Finally, most of the calcium channels of the cell and ER membranes are closed under basal conditions.

Once the dimeric complex $(FGF\text{-}FGFR)_2$ is formed, its Y766 site phosphorylates de Y771 and Y783

sites of PLC [38]. Once PLC is activated, it is translocated to the inner side of the cell membrane and cleavages Phosphatidylinositol-4,5-biphosphate (PIP_2) into inositol-1,4,5-triphosphate (IP3) and diacylglycerol (DAG).

IP3 freely diffuses through the cytoplasm and binds to its specific receptor at the smooth ER membrane, which is a calcium channel [39] (Figure 3). There are three isoforms of the IP3 receptor (IP3R). Each isoform is a tetramer, and each protein of the tetramer has a length of ~ 2749 aa divided into three functional regions. The carboxyl terminal (C-terminal) end of the protein is formed by 6 transmembrane segments and contains the Ca^{2+} channel pore region. The regulatory region of the protein connects the C-terminal end with the amino terminal (N-terminal) end. This regulatory region has ATP binding sites and targets for the phosphorylation of the IP3R by a series of proteins. The IP3 molecule binds to the N-terminal region of the receptor. The three regions project into the cytoplasm [40, 41].

All the IP3R are biphasically regulated by Ca^{2+}. When the cytoplasmic Ca^{2+} concentration is between 100 and 200 nM, the ion exerts a positive feedback loop with the IP3R allowing the liberation of more calcium from the ER store. However, high Ca^{2+} concentration inhibits the IP3R function, contributing to the oscillatory pattern of Ca^{2+} release observed in cells stimulated by agonists like FGF, EGF and Wnt5 [37, 40].

The balance between the rate of Ca^{2+} liberation from the ER stores and the rate of operation of the Ca^{2+} buffering mechanisms produces periodic variations in the cytoplasmic level of this ion that have a frequency proportional to the agonist concentration and a constant amplitude of the order of ~1 μM or more. This characteristic dynamical behavior of the IP3-Ca^{2+} signaling system is named *frequency encoding* and is important in the interpretation of the information from the cell's environment [37, 42, 43].

An additional process is involved in the maintenance of the calcium oscillations in the Xenopus blastomeres. The periodic increase of the calcium levels produces the activation of more phospholipase, closing a positive feedback loop (Figure 3). There are three phospholipase isoforms with different calcium affinity in the Xenopus blastomere: phospholipase Cγ1, phospholipase β and phospholipase δ. From this set of isoforms, the phospholipase δ is activated by calcium at concentrations of the order of 10^{-7} to 10^{-5} M (k_d ~ 30 to 50 μM), this fact sustains the hypothesis that this phospholipase has a role as an amplifier for the calcium signal, while the other two isoforms have a role as initiators of it [44].

4. The Wnt5/Ca^{2+} signaling pathway

4.1. Molecular biology of the Wnt5 signaling pathway

The initial classification of the Wnt proteins was based on their ability to induce a secondary axis with a head, when over-expressed in ventral side of Xenopus embryos. Wnt1, Wnt3a and Wnt8 were able to induce while Wnt4, Wnt5a and Wnt11 were not. The first were referred as canonical, while the latter were called non canonical [45].

It was initially shown that the first group worked through the activation of the β-catenin patheway (canonical), while the second group activated either or both the Wnt/jun N-terminal kinase (JNK) and the Wnt/Ca^{2+} pathways (non canonical) [46]. Now it is known this classification is not as straightforward as it seemed, because individual Wnts can activate both canonical and noncanonical pathways, depending on context [47]. During Xenopus early development, the involvement of both the canonical and non canonical Wnt pathways has been established.

Intracellular calcium levels are regulated by the Wnt/Ca^{2+} pathway, through the binding of Wnt to its receptor Frizzled. Frizzled receptors are seven-transmembrane-spanning molecules, which have an important physiological role during Xenopus development. There are 10 mammalian Fzs (Fz_{1-10}) isoforms with an extracellular N-terminus which contains a cystein-rich domain (CRD domain), three intra- and three extracellular loops, seven transmembrane-spanning helices and an intracellular C-terminal domain that has a highly conserved internal PDZ domain [48]. Frizzled are protein G coupled receptors (PGCR) which are activated by the binding of a Wnt glycoprotein like Wnt5. Once activated, frizzled induces the

cleavage of a coupled heterotrimeric G protein, which releases G_{α} and a $G_{\beta\gamma}$ subunits. $G_{\alpha s}$ activates adenylyl-cyclase (AC) inducing the production of AMPc, while $G_{\alpha i/o}$ inhibits AC and AMPc production. The $G_{\beta\gamma}$ subunit activates PLCβ inducing Ca^{2+} liberation through the IP3-Ca^{2+} signaling pathway. In the case of $G_{\alpha q/11}$, it seems that this subunit can also activate PLCβ concurrently with the $G_{\beta\gamma}$ subunit [44]. PCLβ synergizes with PLCγ in the initiation of the calcium signal. Once the cytoplasmic level of Ca^{2+} is increased, this ion exerts its action through the activation of calcium dependent proteins like calcium/calmodulin-dependent kinase II (CAMKII), protein kinase C (PKC) and calcineurin. Calcineurin produces the activation of the nuclear factor of activated T-cells NFAT and the subsequent activation of NFAT target genes [49]. CAMKII can activate a nemo-like kinase (NLK) that interferes with β-catenin.

5. Calcium dynamics and gene expression in Xenopus MBT blastula

5.1. Single blastomere calcium dynamics

As we pointed out before (see Section 2), in the Xenopus blastomeres of the prospective dorsal ectoderm an intense calcium oscillatory dynamics is set at the MBT stage. Experimental results [38, 44] suggest that this dynamics can be elicited as a result of the co activation of the FGFR and Frizzled receptors.

In order to gain a better insight of the role of these calcium oscillations in the specification of the ventral features of the embryo, it is possible to use a nonlinear dynamics approach. At the moment, the unique mathematical model specifically proposed for the simulation of the single blastomere calcium dynamics at the MBT [43] is based on a two-pool modified model [37, 50, 51]. This model describes the activation of the IP3-Ca^{2+} and the MAPK signaling pathways by FGF.

This model takes into account the following variables: 1) The activation of the FGFR receptor at the cell surface; 2) activation of Raf; 3) activation of PLC; 4) the free calcium concentration in the cytoplasm and 5) the calcium concentration in the ER stores [43, 52]. The set of equations of this model can be consulted in [52].

According to this model, the overall calcium dynamics of the blastomere is determined by three feedback loops (Figure 6). The first feedback loop is set up between calcium and PLC. As we mentioned before (section 3.1), the formation of the dimeric receptor complexes at the cell surfaces triggers the activation of phospholipase C [32] and the subsequent production of IP3 (Figure 3). The IP3 acts on its specific receptor at the endoplasmic reticulum membrane (ER), inducing the flow of calcium from the ER stores to the cytoplasm. This flow of calcium activates a set of damping processes that control the calcium cytoplasmatic level, as well as a set of molecules that can be directly activated by the calcium ion, such as the PKC, CAMKII, NFAT and either of the PLC isoforms (Figure 3). The balance between the process of liberation of calcium by the IP3 and the damping processes can produce an oscillatory behavior of the cytoplasmic calcium levels [42] that are sustained by the continuous Ca^{2+}-dependent activation of more PLC.

The second loop produces a negative feedback due to the activation of Ras by the FGFR dimeric complex through the formation of the Shc–Grb2–SOS complex, and the simultaneous turning on of the GTPase-activating protein (GAP) that damps the amount of active Ras bounded to the inner surface of the plasma membrane.

The third feedback loop is a positive one, which is due to the activation of the Xbra (*Xenopus* brachyury) transcription factor by phosphorylated nuclear ERK [53] (see section 3 and Figure 3,). The dimeric form of the Xbra transcription factor activates the Xbra gene, while its monomeric form activates the XeFGF (*Xenopus* embryonic FGF) gene, closing the positive feedback loop that sustains the mesodermal induction process [54].

These three feedback loops are interconnected by the action of protein kinase C on Raf (Figure 3). The protein kinase C is translocated to the membrane in the presence of dyacil-glycerol (DAG), where it is activated by calcium and enhances Raf activity. Thus, PKC sets a point of crosstalk between the calcium and the MAPK signaling systems. Additionally, there is a difference in calcium responsiveness of the isoforms of PKC located in the embryo. PKC isolated from animal cells of the *Xenopus* blastula is highly sensitive to

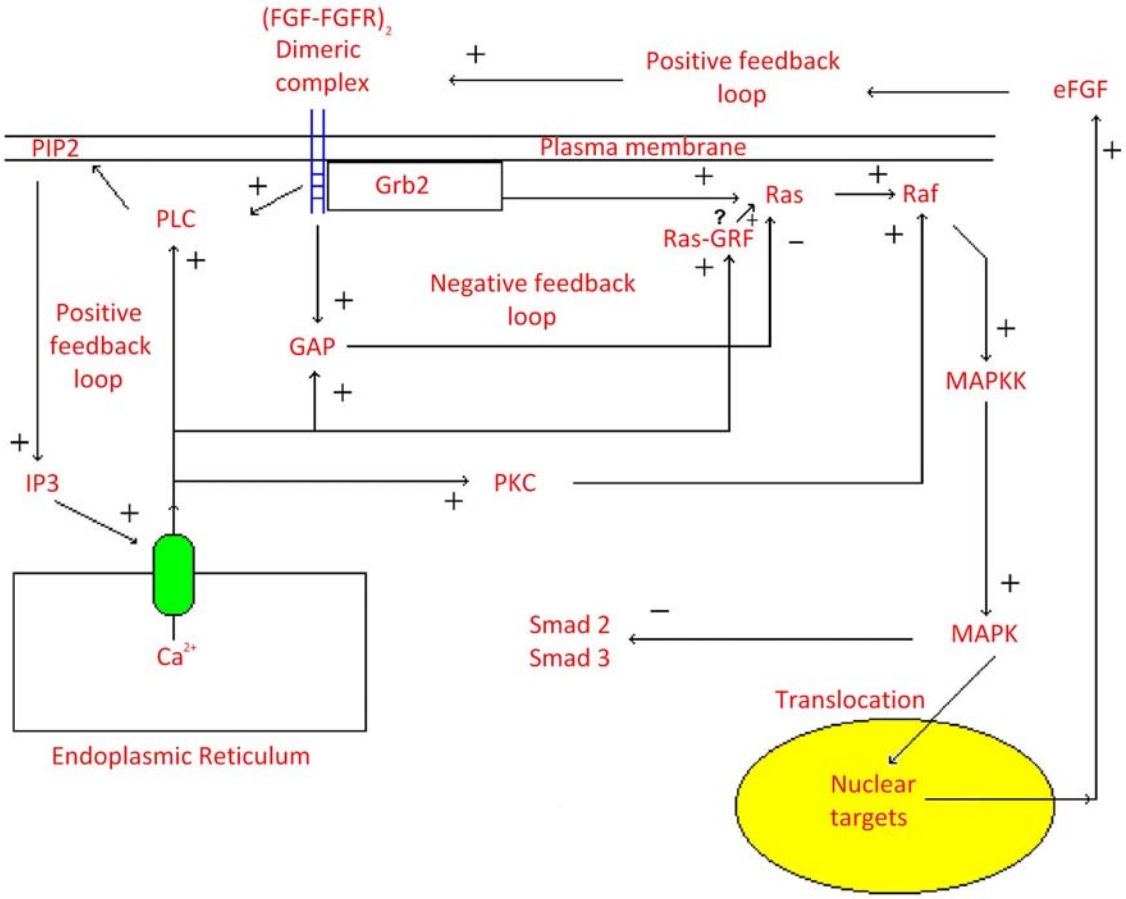

Figure 6. The interaction of the IP3–Ca^{2+} and MAPK signaling system is based on the presence of three feedback loops: 1) a negative feedback loop controls the activation levels of Ras; 2) a positive feedback loop sustains the calcium dynamics. 3) The second positive feedback loop produces more eFGF that is secreted outside the cell, stimulating it and its neighbors. PKC, Ras-GRF and GAP link both Ca^{2+} and MAPK signaling systems. Ras-GRF and PKC enhance the activity of Ras and Raf, respectively, while GAP downregulates Ras activity. The MAPK can block the activin signaling pathways phosphorylating the Smad2 and Smad3 proteins. Grb2 represents the Shc–Grb2–SOS complex in this Figure.

calcium and can also be activated by low concentrations of arachidonic acid, while the PKC isolated from vegetal cells is less sensitive to calcium and cannot be activated by arachidonic acid [55].

A limitation of Díaz and collaborators model [43] is that it does not take into account the regulation of Ras activity by Ca^{2+}. The Ras-guanine-nucleotide-release-factor 1 (Ras-GRF1) and Ras-guanine-nucleotide-release-factor 2 (Ras-GRF2) are points of positive regulation of Ras expression by Ca^{2+}. The molecular mechanism of this interaction seems to lie on the binding of calmodulin to the calmodulin-bindin-IQ-motif of Ras-GRF, regulating the exchange activity of these proteins. Negative points of Ras regulation seem to be the GAP proteins p120-RasGAP and CAPRI. These proteins activate their GTPase activity after an increase of cytoplasmic Ca^{2+} [56].

According to [43], the dynamics of the interaction of the these feedback loops can have one of the following possible effects: 1) if there is not an oscillations in the cytoplasmic calcium levels, then PKC has the effect of enhancing the level of activation of Raf without interfering with the switch-like relay mechanism of the MAPK cascade; 2) if the cytoplasmic calcium level oscillates, but the rate of Raf inactivation is much smaller than

its rate of activation by PKC, then the levels of activation of Raf are enhanced and the MAPK cascade still proceeds as a switch-like relay system; 3) if the cytoplasmic calcium level oscillates and the rate of inactivation of Raf is of the order of its rate of activation by PKC, then PKC can induce an oscillatory behavior in the MAPK cascade giving rise to a frequency encoding mechanism for the control of the Xbra gene expression [52].

Depending on which of these situations takes place in the cell, the calcium oscillatory dynamics may alter the entire dynamics of the MAPK cascade by either adding an oscillatory component to the signal carried by the cascade or modifying the amount of information transmitted to the nucleus during the FGF-dependent induction by increasing the amplitude of the signal [56, 57]. Such a modification of the cascade dynamics can have a direct influence on the expression of genes like Xbra, which is a direct target of the MAPK cascade during the mesodermal induction process [58].

The numerical solution of the Díaz *et al.* model [43], shows that in the blastomere the onset of the oscillatory calcium dynamics after stimulation with FGF is due to a supercritical Hopf bifurcation (see Bifurcations section of the Appendix) that leads to a stable limit cycle in the range of FGF concentrations from ~ 0.16 to ~ 0.30 nM (Figures 7a, 7b and 7c). In this range of concentrations the oscillations have constant amplitude and a frequency proportional to the agonist concentration, i.e., reproduces the frequency encoding property of the signal in an acutely form (see bifurcation diagram in [43]). At a FGF concentration of ~ 0.176 nM the calcium transients have a period of ~ 450 s, which coincides with the experimental values reported in the literature for the period of the calcium transients [19].

As the vesicular traficking of the agonist-receptor complexes and the receptor recycling are not taken into account in this model, the MAPK output signal is a sharp switch like response in absence of calcium, without the initial overshoot transient response reported in other systems [59]. However, in presence of calcium oscillations the MAPK cascade exhibits an oscillatory behavior with a small lag with respect to the Ca^{2+} oscillations (Figure 7d). In this form, it is possible that the blastomeres located at the calcium transients source become stable oscillators.

Unfortunately, Díaz *et al.* model [43] does not explicitly take into account the dynamics of the Wnt5/Ca^{2+} signaling pathway, although it considers in an implicit form the contribution of PLCβ in the balance equation for PLC [52]. However, the information generated by the occupancy of the respective Frizzled receptor by Wnt5 could also have influence on the spatio-temporal pattern of the oscillatory calcium signal generated by the calcium source at the presumptive ectoderm [60].

Experiments using FGFR's mutated at the PCLγ union site are unable of triggering Ca^{2+} efflux from the ER. This mutation does not affect the mesoderm-inducing ability of FGF, indicating that Ca^{2+} is no necessary for mesodermal induction [61, 62], i.e., Ca^{2+} is not an inducing signal but a permissive one that allows the patterning of the mesoderm into the ventral and dorsal sides.

5.2. AM and FM genes

A point of interest that needs clarification is the role of these calcium transients in the determination of the ventralizing features of the Xenopus blastula. Experiments of Dolmetsch *et al.* [58, 63], show that, with respect to their responsiveness to Ca^{2+}, there are two main groups of genes: amplitude modulated (AM) genes and frequency modulated (FM) genes. These genes can respond to the Ca^{2+}- induced regime of temporal variation of the nuclear concentration of the transcription factors that bind to their promoter site.

Dolmetsch and collaborators [63] showed that in self-tolerant B cells, low amplitude steady calcium signals activate the NFAT transcription factor and the ERK pathway, whereas high amplitude steady calcium signals activate NF-κB transcription factor and JNK. Thus, this differential effect of the amplitude of the calcium signal conveys a differential gene expression. Genes that respond to the amplitude of the calcium signal are called AM genes.

In a posterior work [58], by using a controlled calcium oscillator, Dolmetsch and collaborators showed the existence of genes that can respond to the frequency of the induce calcium oscillations in

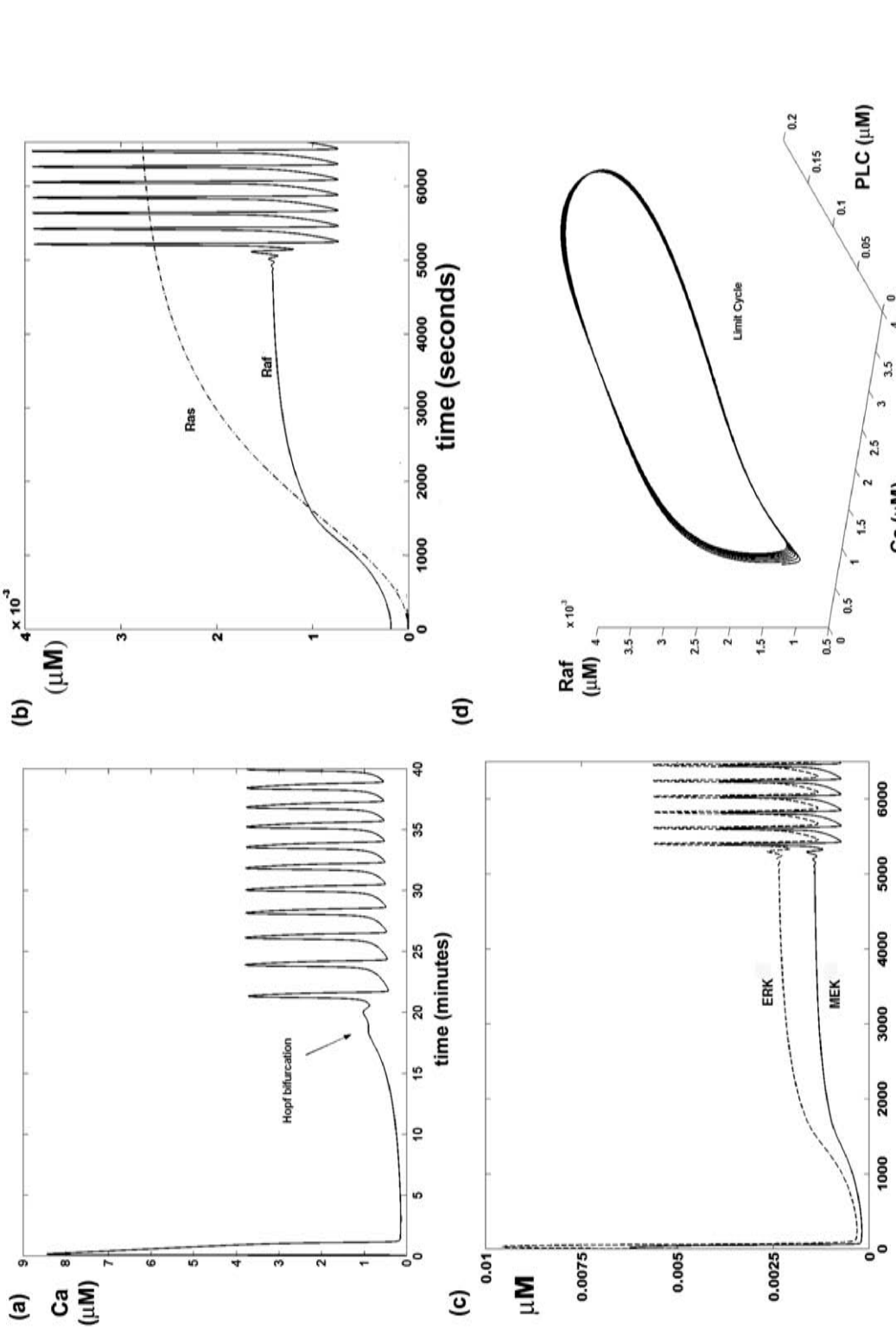

Figure 7. a) When FGF concentration is ~ 0.25 nM, the systems shows a transition from a center, which has two purely imaginary conjugated eigenvalues, to an unstable spiral with two complex conjugated eigenvalues with real positive part [52]. Thus, after a strong transient efflux of calcium from the ER, the system transits to a stable limit cycle though a supercritical Hopf bifurcation, giving rise to Ca^{2+} oscillations with constant amplitude and frequency (see Appendix); b) in this model, Ras has a switch-like behavior but Raf exhibits and oscillatory dynamics due to its interaction with PKC; c) as consequence of Raf oscillatory dynamics, MEK and ERK also exhibits an oscillatory dynamics with the same frequency but with an amplitude that depends on the concentration of each kinase in the blastomere; d) limit cycle in which the components of the MAPK cascade and the IP3-Ca^{2+} signaling pathways interact with each other.

T lymphocytes (Jurkat cells). The transcription factors NF-AT and Oct/OAP are inactivated by calcium signals with a period > 400 s, whereas NF-κB remains active even at periods of ~ 1800 s. Dolmetsch *et al.* [58] also shown, by using transfected cells with luciferase reporter constructs driven by the IL-2 and IL-8 promoters, that the IL-2 gene exhibits the same response pattern that NF-AT and Oct/OAP. In contrast,the IL-8 gene follows NF-κB frequency dependence.

Calcium can also produce a complex dynamics during the translocation of transcription factors into the nucleus. Recent evidence, show that, in yeasts under stress conditions, frequency modulated calcium-dependent bursts of nuclear localization of the transcription factor Crz-1 regulate gene expression. Crz-1 is a calcineurine-zinc finger transcription factor that is desphosphorylated and translocated into the nucleus in response to the concentration of extracellular calcium, which controls the frequency but not the duration of these localization bursts. In the nucleus, Crz-1 induces the gene response of multiple target genes, giving rise to the calcium-stress response of the yeast [64].

In this form, as shown in Figure 3 and discussed in section 2, the blastomeres located in the neighborhood of the calcium transients source are subject to a series of calcium spikes with an average period of 450 s which, according to [58], could shut down the activity of NFAT suppressing its inhibitory effect on β-catenin and favoring the activity of NF-κB.

The NF-κB family of transcription factors is represented in Xenopus by the proteins XrelA and Xrel2 (not shown in Figure 3). Both Xrel2 and XrelA are maternal proteins which are located in the nucleus of the blastomeres of the animal pole from the mid to the late blastula stages [65]. There is an animal-vegetal gradient for XrelA [66] but not for Xrel2 [67]. These proteins have a role in the patterning of the head and tail and in dorso-ventral development [65, 67] by synergizing with β-catenine. In fact, dorsal axis formation driven by β-catenin requires NF-κB activity and vice versa [66]. This action can be reinforced by the positive action of PKC on Dishevelled. However, *this hypothesis needs to be experimentally tested.*

Additionally to the oscillatory calcium dynamics, recent experimental results show that ERK oscillates between the nucleus and the cytoplasm in human mammary epithelial cells under the action of the Epidermal Growth Factor (EGF). The periodicity of these oscillations is of the order of ~ 900 s [68]. These oscillations are proposed to be produced by a negative feedback loop between dually phosphorylated ERK and the MAPK cascade input. Mouse epidermal JB6 cells also show ERK oscillations in response to stimulation with FGF, and these oscillations are robust at a high cell population density, on the contrary of EGF induced oscillations in mammary cells which are damped under low cell population density [68]. Shin *et al.* [69], also report ERK oscillations in COS-1 cells. These oscillations seem to emerge through a supercritical Hopf bifurcation (see Bifurcation section in the Appendix), with a period that depends on the doses of EGF or FGF.

As we mentioned before (Section 5.1), Ca^{2+} could induce Ras oscillations through Ras-GRF1,2 and GAP's proteins [70], and PKC could induce oscillations in the MAPK cascade due to its action on Raf [43]. Thus, it is possible that the blastomeres under the action of FGF can also exhibit ERK oscillations with a period that reflects the period of induced Ras and Raf oscillations (Figure 7). This mechanism of production of ERK oscillations can be complemented by a negative feedback loop between ERK and Raf, producing the down regulation of SOS (not shown in Figure 3) as proposed in [68]. However, there are not experimental data that confirm the existence of ERK oscillations in the blastomeres neither about the influence of these oscillations in the expression of the FGF-XBra-XeFGF loop and other target genes. However, the possibility of existence of these ERK oscillations remains.

5.3. Ca^{2+} flow and ventralization of the Xenopus embryo

At the early stages of Xenopus development gap junctions electrically interconnect all the blastomeres. These gap junctions remain in their open state until the beginning of cell differentiation. In this moment, junctions between cells of the same type remain unclosed, whereas junctions between different cell types close [2, 3].

Ca^{2+} can freely flow through these gap junctions, transmitting information from cell to cell and influencing the gene expression of coupled cells. High-sustained Ca^{2+} concentration can close gap junctions but high transient concentrations do not [71], as consequence periodic calcium signals can be integrally transmitted over a broad area of the embryo forming a network of electrically interconnected cells. Furthermore, molecules like IP3 and AMPc can also diffuse through the gap junctions forming an additional network of chemically interconnected embryonic cells.

Diffusion of IP3 and Ca^{2+} between blastomeres can be modeled with reaction-diffusion equations (see Appendix) of the form:

$$\frac{\partial IP3}{\partial t} = f_1\left(FGF, PLC, IP3, Ca^{2+}\right) + \frac{\partial^2 IP3}{\partial r^2}$$
$$\frac{\partial Ca^{2+}}{\partial t} = f_2\left(FGF, PLC, IP3, Ca^{2+}\right) + \frac{\partial^2 Ca^{2+}}{\partial r^2} \quad (1)$$

subject to suitable boundary conditions. In these equations, functions f_1 and f_2 represents the chemical dynamics of IP3 production and Ca^{2+} liberation from the ER as a function of FGF, PLC, IP3 and Ca^{2+} concentrations.

In the case of the MBT stage, the only mathematical model proposed for describing the flow of Ca^{2+} and IP3 in the embryo is [72]. This model explores the spatio-temporal calcium dynamics on the embryo's surface generated by the calcium source located at the prospective dorsal ectoderm.

In this model, the *Xenopus* MBT blastula is pictured as a sphere of ~ 1 mm of diameter with a total volume of ~ 5.236 x 10^8 μm^3. After the 12th synchronous cell division the embryo has approximately 4096 cells of different size. However, the model assumes that all the cells are spherical and have the same average volume of 127,832 μm^3 and an average diameter of 62.5 μm. Given the fact that the calcium dynamics takes place mainly at the animal pole (Figures 4 and 8a), the model does not take into account the presence of the yolk because the animal cells do not have a significant amount of it. The model is applicable only to the MBT stage of development, because the 13th cell division is asynchronous, and also the above assumptions do not hold for the next stages.

From this sphere, a ring of cells that coincides with the meridian that crosses the calcium source is selected, and cells in this ring are numbered from 1 to 50, starting from the cell located at the top of the ring, in the animal pole (Figure 8b). In this form, cell 8 is the source of the calcium transients.

The spatial localization of the calcium source (Figure 4) does not coincide with the homogeneous distribution of the IP3 along the D-V axis (see Section 2), although most of the IP3R are located at the animal pole [20]. According to [30], FGF is probably distributed evenly over the embryo, as consequence, the spatial distribution of FGF neither account for the localization of this calcium source. As far as we know, there is not experimental data in the literature about the distribution of Wnt5, however, is highly probable that it follows the spatial distribution of other Wnt proteins, which are also evenly distributed on the animal pole of the blastula [30].

Thus, in absence of experimental data about the causes of the spatial localization of the calcium source, the model proposes that all cells are subject to a uniform concentration of FGF as the driven force of the calcium dynamics, and to a spatial over expression of IP3R at the calcium source, modeled by the function:

$$p(\chi) = \begin{cases} e^{-\frac{(\chi-8)^2}{25}} & 1 \le \chi \le 15 \\ 0.1408 & \text{rest of the cells} \end{cases} \quad (2)$$

Where χ represents the distance from cell 1, located at the top of the ring of cells (animal pole), measured in cell diameters. Thus, the maximum of the distribution is located at cell 8 (Figure 8b).

The set of equations of the model for the calcium and IP3 fluxes are [72]:

$$\frac{dPLC^*}{dt} = \frac{k_1 C}{C + k_2} + k_3 Ca - k_4 PLC^* \quad (3)$$

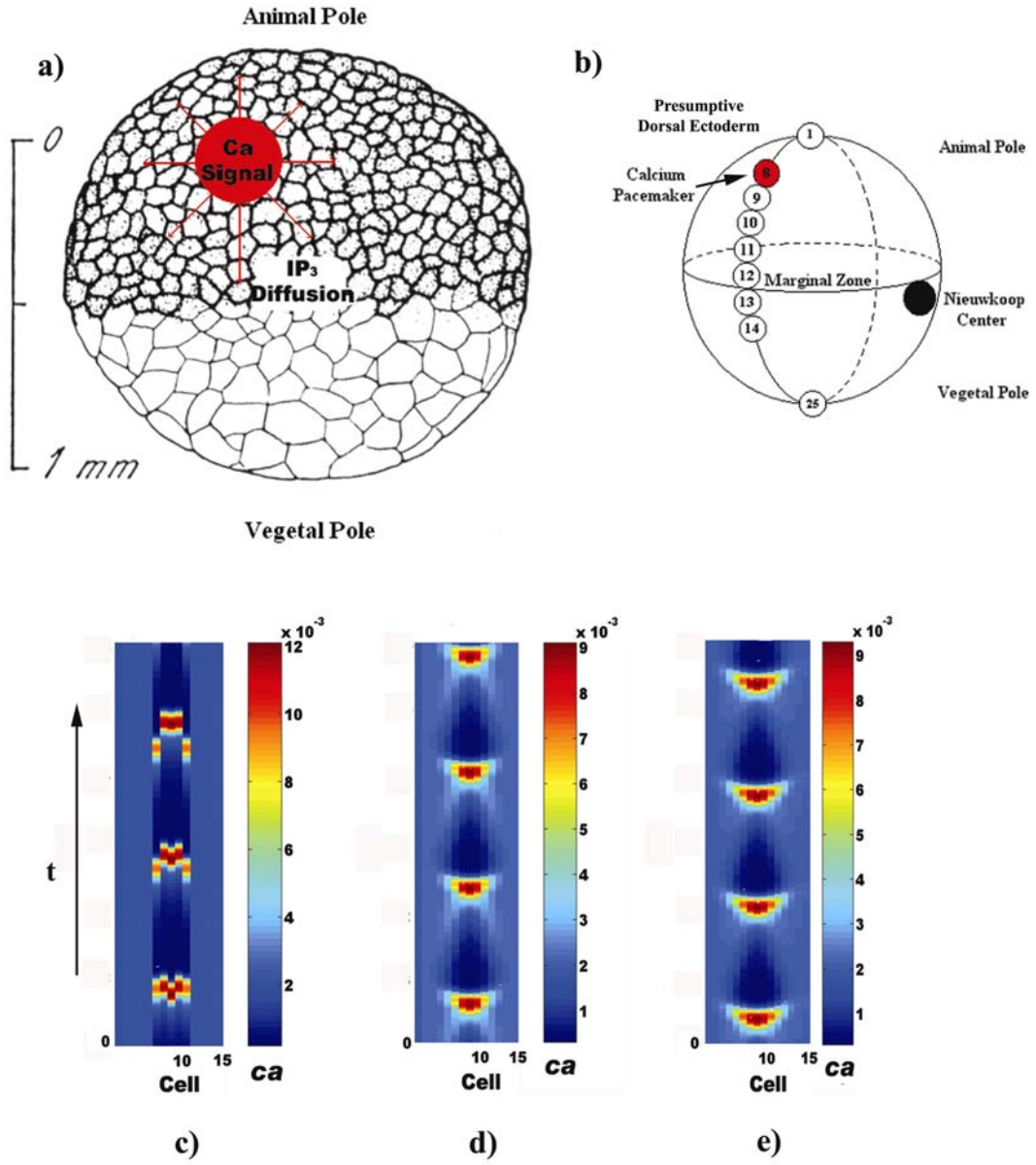

Figure 8. a) The Xenopus blastula at the Mid Blastula Transition state (MBT). At the prospective dorsal ectoderm the calcium source (in red) produces a periodic series of calcium transients. Cells in the neighborhood of the source are coupled by the flow of IP3. The picture of the embryo was reproduced from Leclerc *et al.* [19]; b) if the Xenopus blastula at the MBT is modeled as a sphere, the meridians of the embryo are rings of 1 mm of diameter. This ring can be covered with 50 spherical cells of 62.67 μm of diameter. The cells are numbered counterclockwise; c) when the calcium diffusion coefficient D_{Ca} and the diffusion coefficient of IP3, D_{IP3}, are set to 0, each cell of the ring oscillates at its own rhythm or exhibits a steady calcium concentration, according to its number of IP3R; d) When D_{Ca} = 0 and D_{IP3} = 200 μm^2/s, calcium transients arise in the ring due only to IP3 diffusion. These transients are centered at cell 8 and have a period of ~ 450 s. The amplitude of the transients is ~ 3 μM at cell 8; e) For 0 < D_{Ca} < 50 μm^2/s and D_{IP3} = 200 μm^2/s, as D_{Ca} increases the transients appear in groups conformed by more cells without changing the ~ 450 s period. The amplitude of the transients remains ~ 3 μM at cell 8, while in the rest of the ring cells stay at their respective steady calcium concentration value (cells from 15 to 50, not shown in the figures). In all panels all the cells were subject to 0.176 nM of FGF. In the color bars, red indicates the maximum adimensional calcium concentration and dark blue the minimum value. The x-axis represents the number of the cell and the y-axis the time (*t*) in minutes, which ranges from 0 to 30 min.

$$\frac{dIP_3}{dt} = k_5(IP_{3\,pool} - IP_3)PLC^* - k_6 IP_3 + D_{IP3}\left(IP_3(\chi+1,t) - 2IP_3(\chi,t) + IP_3(\chi-1,t)\right) \quad (4)$$

$$\frac{dCa}{dt} = -\frac{dCaS}{dt} + k_7 PLC^* - k_8 Ca - \frac{k_9 Ca}{Ca + k_{10}} + D_{Ca}\left(Ca(\chi+1,t) - 2Ca(\chi,t) + Ca(\chi-1,t)\right) \quad (5)$$

$$\frac{dCaS}{dt} = -\frac{U^* k_{11} IP3 \cdot Ca \cdot CaS}{(IP3 + k_{12})(Ca + k_{13})} + \frac{k_{14} Ca^2}{Ca^2 + k_{15}} - \frac{k_{16} Ca^2 \cdot CaS}{Ca^2 + k_{17}} \quad (6)$$

$$\frac{dU}{\partial t} = \frac{k_{31}}{k_{32} + Ca^2} - k_{33} U \quad (7)$$

where *Ca* represents the cytoplasmic calcium concentration, *CaS* is the concentration of Ca^{2+} in the ER stores, *PLC** is the concentration of activated phospholipase C, IP_3 is the concentration of IP3 and *U* is represents a parameter that controls the IP3R dynamics. In the original model this equations are complemented with the equations for FGFR and Ras activation [72]. Each one of these variables is a function of the relative cell position (χ) and time *t*. Due to the fact that χ is an adimensional discrete variable, the coupling between cells is represented by the discrete form of the Laplacian. The value of the parameters k_i, i = 1,2,…,33, can be found in [72].

The above set of reaction-diffusion equations are subject to the following boundary and initial conditions:

$$\begin{aligned} &IP_3(50+1,t) = IP_3(1,t) \\ &Ca(50+1,t) = Ca(1,t) \\ &plc(\chi,0) = ip_3(\chi,0) = 0 \\ &Ca(\chi,0) = 0.01\ \mu M \\ &Cas(\chi,0) = 12\ \mu M \end{aligned} \quad (8)$$

the value of D_{IP3} is ~ 200 $\mu m^2/s$, which is sustained as a constant during all the simulations [37] and the D_{Ca} is varied from 0 to 50 $\mu m^2/s$.

The numerical solution of the adimensional form of the model [72] for a FGF spatially uniform concentration of 0.176 nM, with D_{IP3} = 200 $\mu m^2/s$ and D_{Ca} = 31 $\mu m^2/s$, predicts the onset of a periodic calcium dynamics with its source centered at cell 8, and with a period of ~ 450 s (4 calcium transients during the MBT, assuming that the duration of this stage is about 30 min), according to the experimental values (See Figure 8c and 9). This periodic calcium dynamics comprises groups of around 4 cells around cell 8, each one showing a different level of cytoplasmic calcium. Cells numbered from 15 to 50, exhibit a constant low concentration of calcium of ~ 0.75 µM, which is higher than the basal calcium concentration.

One interesting feature of this model is that the diffusion of IP3 along the ring can produce calcium transients even in absence of the flow of calcium (D_{Ca} = 0 $\mu m^2/s$), and create sustained low levels of calcium in cells far from the source (Figure 8b). When $D_{Ca} \neq 0$, the transients show the same spatio-temporal characteristics but extend over a larger number of cells as D_{Ca} increases (Figure 8c, 8d and 8e). When both $D_{IP3} = D_{Ca} = 0$, cell 8 and their neighbors show transients with a period that ranges from 300 to 400 s, and each cell oscillates at its own rhythm depending on the number of IP3R that they have. Thus, the coupling diffusive molecule that synchronizes calcium activity in the embryo could be IP3, which diffuses faster than calcium. The diffusion of IP3 seems to be a necessary and sufficient condition to set on and sustain the calcium dynamics in the embryo. However, *this hypothesis needs experimental verification.*

In this form, the calcium source can synchronize the activity of cells not only in its neighborhood, but also of cells of the ventral side of the embryo in which induces a steady relative low amplitude calcium signal. This steady calcium signal could allow the expression of NFAT, CAMKII and ERK [63 73] blocking the dorsalizing signals from the canonical WNT pathway (Figure 3). However, *this hypothesis needs also to be experimentally tested.*

CONCLUSIONS AND PERSPECTIVES

This review intends not only to be an exhaustive revision of the literature about calcium and the MBT in Xenopus, but tries to integrate this knowledge into a dynamical vision of the role of calcium in the ventralization of the blastula. However, the scarce literature available on the dynamics of calcium at the MBT stage [74] makes

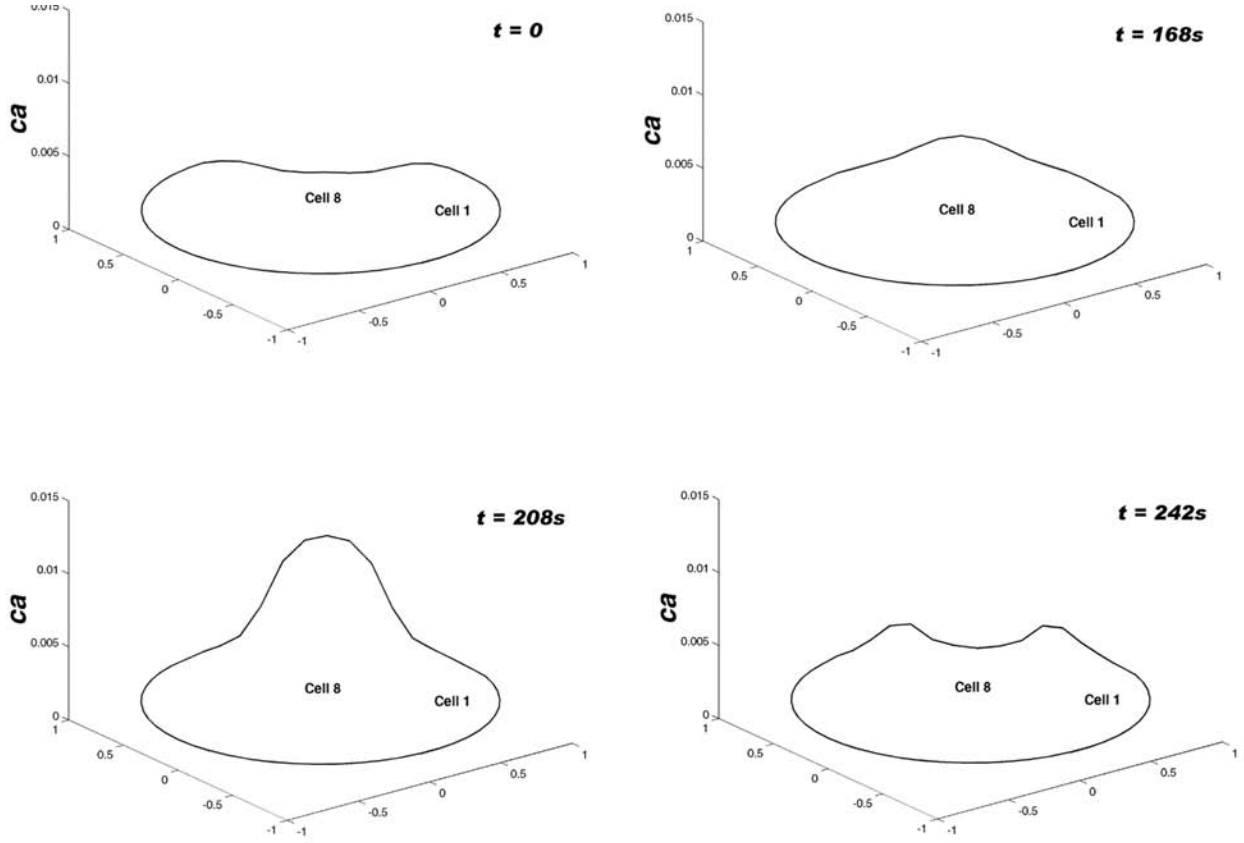

Figure 9. Temporal evolution of the calcium transients of the ring of cells of Figure 8b, subject to a bell-shaped spatial distribution of IP3R. The value of *t* is shown at the upper right corner of each figure. The z-axis represents the adimensional calcium concentration. The x and y axis represent the polar coordinates of each cell. Only the first 242 s of the dynamics are represented.

this objective hard to be reached without falling into speculations. However, this work tries to identify the main unsolved problems and propose a series of hypothesis that can promote further experimental and theoretical research in this field.

From a dynamic point of view, the first problem that requires further experimental and theoretical research is the cause of the restricted spatial localization of the source of the calcium transients. Experimental results on the spatial characteristics of the calcium signal at the MBT show a restricted spatial localization of the source of the signal at a narrow zone of the dorsal ectoderm of the embryo (see Section 2). Neither the spatial distribution of the signaling molecules FGF and Wnt5 nor the spatial distribution of the IP3R explains this fact (see Section 2, Figure 4 and Section 5.3). The model [72], proposes a bell shaped distribution of IP3R around the calcium source in order to reproduce the spatio-temporal characteristics of the calcium transients (see Figure 10). However, this is only a technical assumption to approximate the experimental results.

A possibility asserted by Webb and Miller [74] is that the calcium transients are produced in a stochastic form all over the excitability region. This suggestion implies that small spatial fluctuations in FGF or WNT5 concentrations could be amplified either by stochastic resonance or by the nonlinear chemical processes that drive the IP3 production in the blastomere, giving rise to a differential periodic calcium dynamics. Also, small regional differences in the number of IP3R per cell could account for the observed differences in cell excitability.

However, this proposal could explain the diversity in the amplitude and timing of the calcium transients observed in the embryo but not the causes of the

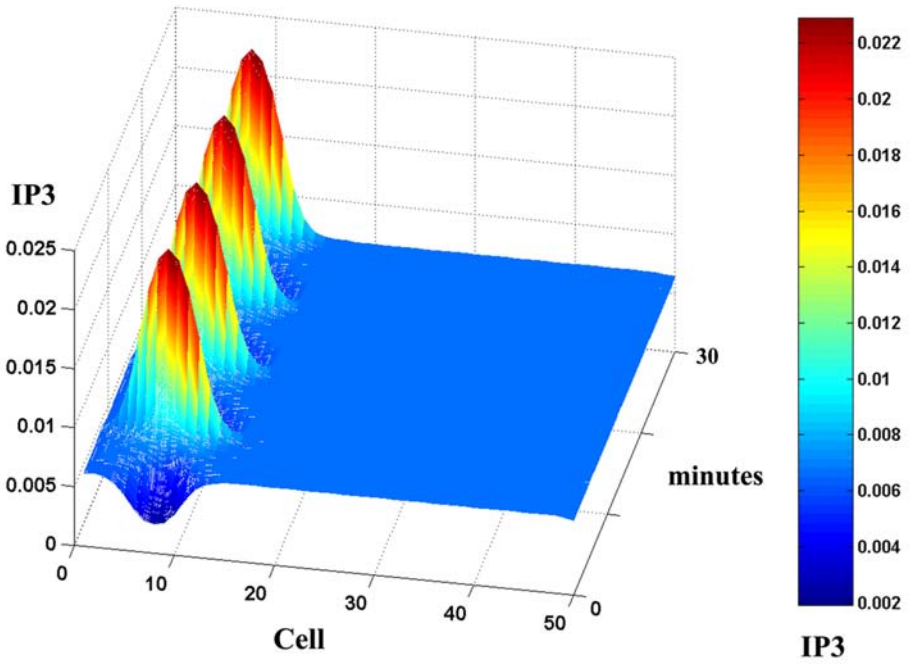

Figure 10. IP3 transients in the ring of cells shown in Figure 8b, under stimulation with 0.176 nM of FGF. The z-axis represents the adimensional IP3 concentration, x-axis the number of the cell in the ring and y-axis the time in minutes. The color bar represents the equivalence between the IP3 concentration and the colors of the figure. Color red represents the maximum IP3 concentration and color blue the minimum IP3 concentration.

regionalization of these fluctuations. Further experimental and theoretical research is needed to identify the causes of this spatial distribution of the signal and of the high calcium excitability of these blastomeres.

From a dynamical point of view, a second problem is the form in which this signal induces the ventralization of the embryo, and in particular, of the mesoderm. Experimental results of Kume *et al.* [44], clearly show that the blockage of the IP3R induces the dorsalization of the embryo [44, 60] (Figure 3), but Leclerc *et al.* [19] show that the calcium transients arise at the dorsal side of the ectoderm. A possible hypothesis to explain these paradoxical results lies on a possible dual function of the calcium signal, i.e., it is a permissive signal that allows the action of the ventral inducting signals in the embryo and synergizes with dorsalizing signals in the dorsal ectoderm.

The spatio-temporal properties of the calcium signal and the experimental findings of Dolmetsch *et al.*, sustain this hypothesis [58, 63]. Although there are not data available about the frequency dependence of Xenopus genes, the existence of the NF-κB family of transcription factors and NFAT in the Xenopus blastomeres at the MBT (Figure 3) opens the possibility that their frequency response properties are very similar to that of their homologues in Jukart and lymphocyte B cells.

If this is the case, there is a cut off period of the calcium signal of about ~ 400 s at which NFAT is turned off and NF-κB continues active. NF-κB and β-catenin co activate genes like Xenopus nodal related 3 (Xnr3) which is a dorsally expressed gene [66]. Thus, it is possible that at the presumptive dorsal ectoderm the calcium transients block NFAT activity and favors NF-κB action.

On the contrary, the expression of either NF-AT or NF-κT could be determined by the amplitude of the calcium signal in the embryo zones without calcium transients [63]. As it was pointed out before (Section 5.3), Diaz *et al.* [72] model proposes that IP3 could be the diffusible molecule that coordinates calcium dynamics even in cells far from the calcium source. Beside the limitations of this model, this suggestion could explain how a dorsal signal induces a ventralizing one.

IP3 diffuses faster than calcium and rapidly reaches all cells in the ring of blastomeres (Figure 10), inducing a steady low calcium concentration of ~ 0.750 μM, which, assuming that Dolmetsch *et al.* results [63] hold also for the Xenopus blastomeres, may drive NFAT-dependent blockage of the canonical Wnt pathway, allowing the expression of ventralizing features and mesoderm induction by FGF due to the fact that ERK activity is also enhanced under this condition. This could explain Kume *et al.* [44] experimental results in which the blockage of IP3R allows the dorsalization of the embryo. At the dorsal side, suppression of the calcium signal would allow a high dorsalizing NF-κB-independent activity of β-catenin, which forms transcription complexes with the TCF family of transcription factors (Figure 3).

The dynamical spatio-temporal characteristics of the cross-talk between the signaling pathways that are active at the MBT transition stage (Figure 3) creates a third problem that is necessary to clarify in order to understand how these molecules can drive the transition to late blastula and gastrulation (see Section 1). Although the molecular actors are known, the form in which they exert their action is just beginning to be known [4]. This network of molecular interactions is complex in the sense that the actors can perform different roles, even opposite ones. For example, Dishevelle can unlock β-catenin in the canonical Wnt pathway but also can drive Ca^{2+} dynamics when Wnt5 activates Fz5 receptor [75]. Furthermore, Dishevelle can also exert a positive action on Ras enhancing the FGF driven inducting activity of the MAPK. PKC can also exert a positive action on Dishevelle (Figure 3). In this form, it could be of great interest the modeling of these interactions in order to characterize the form in which the topology of the network determines its different forms of operation in time and space. This knowledge will be useful to get a better insight on how the regional differentiation of the blastula starts at the MBT stage.

MBT determines the onset of the zygotic genetic activity driven by the presence of maternal molecules that also pattern the mid blastula into different zones with different fate. Although the duration of this stage is about ~ 30 min, a great number of molecular events occur in this short interval of time. As result, the synchrony in cell division is broken due to a differential rate of cell division between animal and vegetal blastomeres. Furthermore, each cell acquires different competence to respond to the inductive signals according to its relative position in the blastula (see Section 1 and Figure 2) and, possibly, to the respective output produced by the balance between the set of intracellular chemical processes represented in Figure 3.

In this process of differentiation, calcium takes an important role as a permissive long-distance signal that coordinates global and localized developmental processes. Thus, further experimental and theoretical research is necessary to understand how calcium interacts with the pattern of inductive signals (Figure 2) to drive the developmental events that allow the successful transition of the Xenopus embryo from the MBT to later stages.

ACKNOWLEDGMENTS

We thank Erika Juarez Luna for technical and logistical assistance. Financial support for this work was from CONACYT (Consejo Nacional de Ciencia y Tecnología) grant 105678.

REFERENCES

1. Harland, R. and Gerhart, J. 1997, Annu. Rev. Cell. Dev. Biol., 13, 611.
2. Wolpert, L. and Tickle, Ch. 2010, Principles of Development, Oxford University Press, New York.
3. Slack, J. 2001, Essential Developmental Biology, Wiley-Blackwell, Oxford.
4. Heasman, J. 2006, Development, 133, 1205.
5. Kofron, M., Demel, T., Xanthos, J., Lohr, J., Sun, B., Sive, H., Osada, S., Wright, C., Wylie, C. and Heasman, J. 1999, Development, 126, 5759.
6. Schulte-Merker, S. and Smith, J. C. 1995, Current Biology, 5, Issue 1, 62-67.
7. Heasman, J. 1997, Development, 124, 4179.
8. Latinkic´, B., Umbhauer, M., Neal, K., Lerchner, W., Smith, J. and Cunliffe, V. 1997, Genes & Development, 11, 3265.
9. Schulte-Merker, S. and Smith, J. C. 1995, Current Biology, 5, 62.

10. Hayward, P., Kalmar, T. and Arias, A. M. 2008, Development, 135, 411.
11. Verheyen, E. M. and Gottardi, C. J. 2010, Dev. Dyn., 239, 34.
12. Nusse, R. 2005, Cell Research, 15, 28.
13. Clements, W. K. and Kimelman, D. 2007, Analysis of Canonical Wnt signaling in Xenopus Embryo. Whitman, M. and Sater, A. (Ed.), CRC Press, New York.
14. Kumano, G. and Smith, W. C. 2000, Dev. Biol., 228, 304.
15. Xu, R. H., Ault, K. T., Kim, J., Park, M. J., Hwang, Y. S., Peng, Y., Sredni, D. and Kung, H. 1999, Dev. Biol., 208, 352.
16. Pera, E. M., Ikeda, A., Eivers, E. and De Robertis, E. M. 2003, Genes Dev., 17, 3023.
17. Kühl, M., Sheldahl, L. C., Malbon, C. C. and Moon, R. T. 2000, J. Biol. Chem. a, 275, 12701.
18. Lee, S. Y. and Lim, S. Y. 2011, Differentiation, 82, 99.
19. Leclerc, C., Webb, S. E., Daguzan, C., Moreau, M. and Miller, A. L. 2000, Journal of Cell Science, 113, 3519.
20. Kume, S., Muto, A., Okano H. and Mikoshiba K. 1997, Mech. Dev., 66, 157.
21. Kume, S. 1999, Cell. Mol. Life Sci., 56, 296.
22. Ault, K. T., Durmowicz, G., Galione, A., Harger, P. L. and Busa, W. B. 1996, Development, 122, 2033.
23. Böttcher, R. T. and Niehrs, C. 2005, Endocr. Rev., 26, 63.
24. Mohammadi, M., Olsen, S. K. and Ibrahimi O. A. 2005, Cytokine Growth Factor Rev., 16, 107.
25. Gillespie, L. L., Paterno, G. D. and Slack, J. M. 1989, Development, 106, 203.
26. Gotoh, N. 2008, Cancer Sci., 1319, 1325.
27. Dailey, L., Ambrosetti, D., Mansukhani, A. and Basilico, C. 2005, Cytokine Growth Factor Rev., 16, 233.
28. Olsen, S. K., Garbi, M., Zampieri, N., Eliseenkova, A. V., Ornitz, D. M., Goldfarb, M. and Mohammadi, M. 2003, J. Biol. Chem., 278, 34226.
29. Goldfarb, M., Schoorlemmer, J., Williams, A., Diwakar, S., Wang, Q., Huang, X., Giza J., Tchetchik, D., Kelley, K., Vega, A., Matthews, G., Rossi, P., Ornitz, D. M. and D'Angelo, E. 2007, Neuron, 55, 449.
30. Schohl, A. and Fagotto, F. 2002, Development, 129, 37.
31. Klint, P. and Claesson-Welsh, L. 1999, Front Biosci., 15, D165.
32. Ryan, P. J. and Gillespie, L. L. 1994, Dev. Biol., 166, 101.
33. Garrington, T. P. and Johnson, G. L. 1999, Curr. Opin. Cell Biol., 11, 211.
34. Karp, G. 1999, Cell and Molecular Biology, Wiley, New York.
35. Heasman, J. 2006, Development, 133, 1205.
36. Vonica, A., Barry, M. and Gumbiner, B. M. 2002, Developmental Biology, 250, 112.
37. Keener, J. and Sneyd, J. 1998, Mathematical Physiology, Springer-Verlag, New York.
38. Rebecchi, M. J. and Pentyala, S. N. 2000, Physiol. Rev., 80, 1291.
39. Miyasaki, S. 1995, Curr. Opin. Cell. Biol., 7, 190.
40. Patterson, R. L., Boehning, D. and Snyder, S. H. 2004, Annu. Rev. Biochem. , 73, 437.
41. Aidley, D. J. and Stanfield, P. R. 1996, Ion channels: molecules in action, Cambridge University Press, Cambridge.
42. Kummer, U., Olsen, L. F., Dixon, C. J., Green, A. K., Bornberg-Bauer, E. and Baier, G. 2000, Biophys. J., 79, 1188.
43. Díaz, J., Baier, G., Martínez-Mekler, G. and Pastor, N. 2002, Biophys. Chem., 97, 55.
44. Kume, S., Inoue, T. and Mikoshiba, K. 2000, Dev. Biol., 226, 88.
45. Du, S. J., Purcell, S. M., Christian, J. L., McGrew, L. L. and Moon, R. T. 1995, Mol. Cell. Biol., 15, 2625.
46. Kikuchi, A., Yamamoto, H. and Kishida, S. 2007, Cell Signal., 19, 659.
47. Cha, S., Tadjuidje, E., Tao, Q., Wylie, C. and Heasman, J. 2008, Development, 135, 3719.
48. Komiya, Y. and Habas, R. 2008, Organogenesis, 4, 68.
49. Rao, T. P. and Kühl, M. 2010, Circulation Research, 106, 1798.
50. Dupont, G., Berridge, M. J. and Goldbeter, A. 1991, Cell Calcium, 12, 73.
51. Dupont, G. and Croisier, H. 2010, HFSP J., 4, 43.
52. Díaz, J. and Martínez-Mekler, G. 2005, Bulletin of Mathematical Biology 67, 433.
53. Curran, K. L. and Grainger, R. M. 2000, Dev. Biol., 228, 41.

54. Casey, E. S., O'Reily, M. A., Conlon, F. L. and Smith, J. C. 1998, Development 125, 3887.
55. Otte, A. P., Kramer, I. M., Mannesse, M., Lambrechts, C. and Durston, A. J. 1990, Development, 110, 461.
56. Cullen, P. J. and Lockyer, P. J. 2002, Molecular Cell Biology, 3, 339.
57. González-García, J. S. and Díaz, J. 2011, Plant Signaling & Behavior, 6, 1.
58. Dolmetsch, R. E., Xu, K. and Lewis, R. S. 1998, Nature, 392, 933.
59. Yamada, S., Taketomi, T. and Yoshimura, A. 2000, Biochemical and Biophysical Research Communications, 314, 1113.
60. Whitaker, M. 2006, Physiol. Rev., 86, 25.
61. Muslin, A. J., Peters, K. G. and Williams, L. T. 1994, Mol. Cell Biol., 14, 3006.
62. Slusarski, D. C. and Pelegri, F. 2007, Developmental Biology, 307, 1.
63. Dolmetsch, R. E., Lewis, R. S., Goodnow, C. C. and Healy, J. I. 1997, Nature, 386, 855.
64. Cai1, L., Dalal, C. K. and Elowitz, M. B. 2008, Nature, 455, 485.
65. Beck, C. W., Sutherland, D. J. and Woodland, H. R. 1998, Int. J. Dev. Biol., 42, 67.
66. Armstrong, N. J., Fagotto, F., Prothmann, C. and Rupp, R. A. W. A. 2012, PLoS ONE, 7, e36136.
67. Tannahil, D. and Wardle, F. C. 1995, Int. J. Dev. Biol., 39, 549.
68. Weber, T. J., Shankaran, H., Wiley, H. S., Opresko, L. K., Chrisler, W. B. and Quesenberry, R. D. 2010, J. Invest. Dermatol., 130, 1444.
69. Shin, S., Rath, O., Choo, S., Fee, F., McFerran, B., Kolch, W. and Cho, K. 2009, Journal of Cell Science, 122, 425.
70. Li, W., Llopis, J., Whitney, M., Zlokarnik, G. and Tsien, R. 1998, Nature, 392, 936.
71. Rottingen, J. A. and Iversen, J. G. 2000, Acta Physiol. Scand., 169, 203.
72. Díaz, J., Pastor, N. and Martínez-Mekler, G. 2005, Developmental Dynamics, 232, 301.
73. Berridge, M. J. 1997, Nature, 386, 759.
74. Webb, S. E. and Miller, A. L. 2006, Biochim. Biophys. Acta., 1763, 1192.
75. Sheldahl, L. C., Slusarski, D. C., Pandur, P., Miller, J. R., Kühl, M. and Moon, R. T. 2003, The Journal of Cell Biology, 161, 769.

APPENDIX

Nonlinear cell dynamics

Xenopus blastomeres are complex networks of physicochemical processes that support their epigenetic changes in structure and function during development. Thus, each cellular process sustained by a blastomere involves different levels of cellular organization. Each level of organization can be represented as a cell subsystem (subnetwork) that functions in a modular mode [1, 2]. In this form, blastomeres can be modeled as formed by a set of subsystems like the regulatory genetic network, the network of synthesis and distribution of proteins, the network of signaling pathways, and the metabolic network, among others.

The information flow through the set of cellular subsystems that controls the cell response to environmental signals occurs according to the canonical schema of Figure A1. An important remark from this Figure is that the flow of information through cellular subsystems is due to a continuous flow of matter and energy, according to the respective laws of conservation. Taking into account the flow of matter at each point of the cell, the respective mass balance equation is:

$$\frac{\partial x_k(\mathbf{r},t)}{\partial t} = \sum_j \nu_{jk} \cdot \omega_j \left(x_1(\mathbf{r},t) x_2(\mathbf{r},t) ... x_k(\mathbf{r},t) ... x_s(\mathbf{r},t) \right) + D_k \nabla^2 x_k(\mathbf{r},t) \quad (1)$$

which means that the local rate of variation of the concentration of the substance *k* (denoted by x_k) at point **r** at time *t* is equal to the net rate of diffusion of *k* inside the cell volume *V* (denoted by $D_k \nabla^2 x_k(\mathbf{r},t)$) plus the rate of formation/ degradation of *k* due to the local chemical reactions inside *V*. In equation (1), ω_j represents the local rate of the chemical reaction *j*, which is a functional of the concentration of the reactive substances at point **r** at time *t*, and ν_{jk} is the stoichiometric coefficient of *k* in reaction *j*.

The reaction term of equation (1) can be rewritten as:

$$\sum_j \nu_{jk} \cdot \omega_j \left(x_1(\mathbf{r},t), x_2(\mathbf{r},t) ... x_k(\mathbf{r},t) ... x_s(\mathbf{r},t) \right) = f_k \left(x_1(\mathbf{r},t), x_2(\mathbf{r},t), ..., x_k(\mathbf{r},t), ... x_s(\mathbf{r},t) \right) \quad (2)$$
$$k = 1, 2, ..., s$$

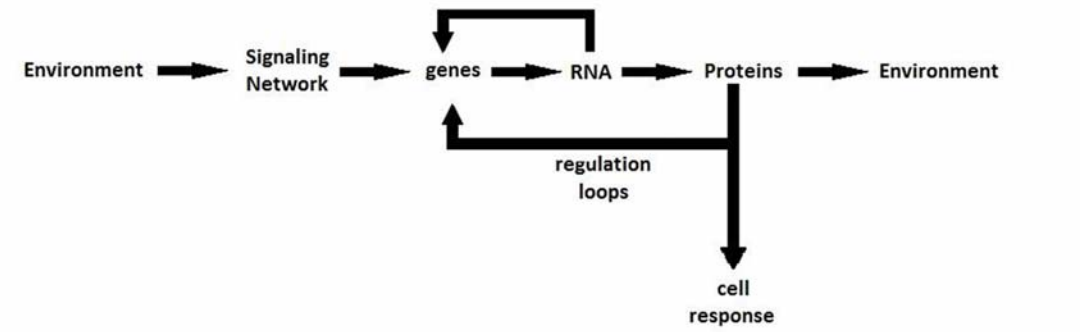

Figure A1. Changes in environmental conditions are sensed by cell signaling networks, which code and transmit this information to the nucleus. Coded information is decoded by the transcription machinery that, in response to this information, activates and inactivates a set of specific genes, giving rise to a precise distribution of effector proteins. These proteins induce a cellular response to the environmental conditions. Some of these proteins can be used to regulate gene expression, acting as specific transcription factors that form complex regulatory loops inside the nucleus. Proteins can also be secreted to modify the cell environment. Tumor-inducing viral RNA and DNA can modify this flow of information by acting directly on the cell genome, drastically modifying the population of effector proteins and their function.

leading to:

$$\frac{\partial x_k(\mathbf{r},t)}{\partial t} = f_k\left(x_1(\mathbf{r},t), x_2(\mathbf{r},t), ..., x_k(\mathbf{r},t), ...x_s(\mathbf{r},t)\right) + D_k\nabla^2 x_k(\mathbf{r},t) \quad k = 1,2,...,s \tag{3}$$

which is the well known form of the reaction-diffusion equation for the substance *k*. It indicates that the temporal variation of the concentration of *k* at point **r** at time *t* depends on the balance between the chemical processes in which this substance takes part, represented by the function f_k, and its diffusion rate in the cellular medium. Function f_k is generally a nonlinear function of the concentration of the reactive substances, and equation (3) usually has not an analytical solution. In a homogeneous medium the diffusive term in equation (3) is null, and f_k completely defines the entire system dynamics in the *s*-dimensional phase space, which is defined by the set of concentration values of the *s* reactive substances.

The systems dynamics is represented by a trajectory in this space, defined by the column vector $\mathbf{x}^o = \begin{bmatrix} x_1^0 \\ x_2^0 \\ \vdots \\ x_s^0 \end{bmatrix}$. In nonlinear systems this trajectory can have peculiar characteristics like high sensitivity to initial conditions, bifurcations and complex loops that represent a great variety of dynamical behaviors observed in biological systems like limit cycles, hysteresis, bistability, ultrasensitivity, among others. In not homogeneous medium the diffusive term of equation (3) produces a more complex dynamical behavior of the system, giving rise to phenomena like traveling waves, spirals and spatially located bursting of second messengers and proteins, among others.

Stability of nonlinear systems

The first problem concerning the dynamics of nonlinear systems is the determination the steady points of the system in its phase space. We consider at this point the case of a homogeneous chemical system.

A steady point is a column vector $\mathbf{x}^o = \begin{bmatrix} x_1^0 \\ x_2^0 \\ \vdots \\ x_s^0 \end{bmatrix}$ for which the equation:

$$\dot{\mathbf{x}}(t) = \mathbf{f}\left(\mathbf{x}(t)\right), \quad \text{where } \mathbf{f}\left(\mathbf{x}(t)\right) = \begin{bmatrix} f_1\left(x_1(t), x_2(t), ...x_k(t), ...x_s(t)\right) \\ \vdots \\ f_s\left(x_1(t), x_2(t), ...x_k(t), ...x_s(t)\right) \end{bmatrix} \tag{4}$$

becomes zero. Once the set of steady points of the system is settled, it is necessary to determine the stability of each steady point. Equation (4) subject to the initial condition $\mathbf{x}(0)=\mathbf{x}_0$ defines a nonlinear dynamical system.

The steady point $\mathbf{x}^o$ of a dynamical system is Liapunov stable if for each $\varepsilon > 0$ exits a $\delta > 0$ such that:

$\left\|\mathbf{x}(t)-\mathbf{x}^o\right\| < \varepsilon$ whenever $\left\|\mathbf{x}(0)-\mathbf{x}^o\right\| < \delta$, i.e., any trajectory that initiates at a distance δ of the steady point $\mathbf{x}^o$ remains at a distance ε of it for all positive time.

The steady point $\mathbf{x}^o$ of a dynamical system is attracting if exists a $\delta > 0$ such that $\lim_{t\to\infty}\mathbf{x}(t)=\mathbf{x}^o$ for any trajectory $\mathbf{x}=\mathbf{x}(t)$ whenever $\left\|\mathbf{x}(0)-\mathbf{x}^o\right\| < \delta$, i.e., any trajectory that initiates at a distance δ of the steady point $\mathbf{x}^o$ will converge to it eventually. In this case, the point $\mathbf{x}^o$ is an attractor of the dynamical system in the phase space. A steady point $\mathbf{x}^o$, which is Liapunov stable and attracting, is asymptotically stable.

A steady point $\mathbf{x}^o$, which is neither stable nor attracting, is unstable and is a repulsor in the phase space.

Phase plane analysis

In nonlinear systems the trajectories cannot be generally determined in an analytical form. However, it is possible to perform a qualitative analysis to find out the global behavior of the dynamical system in the corresponding phase space. As a vector can be assigned to each point of this space, according to equation (4), the vector field associated to the phase space can be drawn. By flowing this vector field, a phase point traces a solution $\mathbf{x}(t)$ of the dynamical system, corresponding to a trajectory winding through the phase space.

It is of importance to point out the fact that if the function $\mathbf{f}$ of equation (4) is continuous and all its partial derivates $\frac{\partial f_i}{\partial x_j}$ $i, j = 1,2,...,s$ are also continuous in $\mathbf{x}$ for a given subset $D \subset \Re^n$, then for every $\mathbf{x}_0 \in D$ the initial value problem of equation (4), has solution $\mathbf{x}(t)$ in some time interval $(-t,t)$ around $t = 0$ and this solution is unique. A topological implication of this theorem is that two trajectories cannot intersect and, as consequence, chaos is ruled out of any 2-dimensional phase space but arises as a possible behavior of every s-dimensional dynamical system with s > 2 [3].

The phase space analysis of the dynamics of a nonlinear system takes into account the following aspects: 1) the number, position and stability of the steady points; 2) the arrangement of the trajectories near the steady points; and 3) the existence and stability of closed orbits.

In the previous section was presented the form in which the steady points are determined and how they can be classified according to their stability. The arrangement of the trajectories around steady points is determined by linearization of the original nonlinear system, and analysis of the behavior of the eigenvalues of the Jacobian matrix of the linearized system around each steady point. For example, considering a 2-dimensional phase space and a steady point $\mathbf{x}^o = \begin{bmatrix} x_1^o \\ x_2^0 \end{bmatrix}$, a small perturbation from this steady state drives the nonlinear dynamical system $\begin{bmatrix} \dot{x}_1(t) \\ \dot{x}_2(t) \end{bmatrix} = \begin{bmatrix} f_1\left(x_1(t), x_2(t)\right) \\ f_2\left(x_1(t), x_2(t)\right) \end{bmatrix}$ into a new trajectory $\delta\mathbf{x}(t) = \begin{bmatrix} \delta x_1(t) \\ \delta x_2(t) \end{bmatrix}$, where $\delta x_1(t) = x_1(t) - x_1^o$ and $\delta x_2(t) = x_2(t) - x_2^o$. In this form:

$$\begin{aligned}\delta\dot{x}_1 = \dot{x}_1 &= f_1(x_1^o, x_2^o) + \left.\frac{\partial f_1}{\partial x_1}\right|_{(x_1^o, x_2^o)} \delta x_1 + \left.\frac{\partial f_1}{\partial x_2}\right|_{(x_1^o, x_2^o)} \delta x_2 \\ &\quad + O\left(\delta^2 x_1, \delta^2 x_2, \delta x_1 \delta x_2\right) \\ &= \left.\frac{\partial f_1}{\partial x_1}\right|_{(x_1^o, x_2^o)} \delta x_1 + \left.\frac{\partial f_1}{\partial x_2}\right|_{(x_1^o, x_2^o)} \delta x_2 \\ &\quad + O\left(\delta^2 x_1, \delta^2 x_2, \delta x_1 \delta x_2\right)\end{aligned}$$

because $f_1(x_1^o, x_2^o) = 0$

(5)

In a similar form:

$$\delta\dot{x}_2 = \dot{x}_2 = \left.\frac{\partial f_2}{\partial x_1}\right|_{(x_1^o, x_2^o)} \delta x_1 + \left.\frac{\partial f_2}{\partial x_2}\right|_{(x_1^o, x_2^o)} \delta x_2 + O\left(\delta^2 x_1, \delta^2 x_2, \delta x_1 \delta x_2\right) \quad (6)$$

which leads to the linearized dynamical system:

$$\begin{bmatrix} \delta\dot{x}_1(t) \\ \delta\dot{x}_2(t) \end{bmatrix} = \begin{bmatrix} \left.\frac{\partial f_1}{\partial x_1}\right|_{(x_1^o, x_2^o)} & \left.\frac{\partial f_1}{\partial x_2}\right|_{(x_1^o, x_2^o)} \\ \left.\frac{\partial f_2}{\partial x_1}\right|_{(x_1^o, x_2^o)} & \left.\frac{\partial f_2}{\partial x_2}\right|_{(x_1^o, x_2^o)} \end{bmatrix} \begin{bmatrix} x_1(t) \\ x_2(t) \end{bmatrix} = \mathbf{J}\left[x_1, x_2\right] \begin{bmatrix} x_1(t) \\ x_2(t) \end{bmatrix} \quad (7)$$

$\mathbf{J}\left[x_1, x_2\right]$ represents the Jacobian matrix of the linearized dynamical system in equation 6. The eigenvalues λ_1, λ_2 of $\mathbf{J}\left[x_1, x_2\right]$ can be calculated from the characteristic equation: $\left|\mathbf{J}\left[x_1, x_2\right] - \lambda\mathbf{I}\right| = 0$. Depending on the nature of the eigenvalues, it is possible to know the arrangement of the trajectories near each steady point of the nonlinear system (Figure A2). This linearization process can be extended to perform the phase space analysis of higher dimensional nonlinear dynamical systems [4].

When the eigenvalues of the Jacobian matrix are pure imaginary $\lambda = \pm i$, the steady point is a center. The trajectories around this point are closed orbits that are stable. However, the neglected nonlinear terms in equations (5) and (6) can produce an imperfect closure of the orbit, giving rise to a spiral. In this form, the vector field corresponding to a center is altered by small nonlinear perturbations that transform the center into a spiral and, as consequence, has not structural stability [3].

According to their stability, steady points of 2-dimensional dynamical systems can be classified into a: 1) Robust case, which includes repellers or sources, for which both eigenvalues have Re(λ) > 0; attractors or sinks, for which both eigenvalues have Re(λ) < 0 and saddles, for which one eigenvalues has Re(λ) > 0 and the other one has Re(λ) < 0; 2) Marginal case, which includes centers for which both eigenvalues are pure imaginary, and non-isolated steady points for which one eigenvalue has Re(λ) = 0 [3].

However, the phase space of a nonlinear system can exhibit another kind of closed orbits called limit cycles, which cannot be observed in linear systems. A limit cycle is an isolated trajectory for which neighbor trajectories can be only spirals that converge to it or diverge from it. If all the spirals converge into the limit cycle, this closed orbit is stable, otherwise is unstable. The existence of this kind of closed trajectories in the plane is settled down by the Poincaré-Bendixson theorem. According to this theorem, exits a trajectory C, which is either a closed orbit or a spiral that converges to a closed orbit as $t \to \infty$, confined inside a certain closed bounded region R of the plane. This theorem assumes 1) the existence of a vector field $\dot{\mathbf{x}} = \mathbf{f}(\mathbf{x})$ that is continuously differentiable on an open set of the plane containing R and 2) R does not contain any fixed point [4]. A consequence of this theorem is that in a 2-dimensional phase space any trajectory trapped into a closed bounded region R must converge to a limit cycle.

However, in higher dimensional systems the Poincaré-Bendixon theorem does not longer apply and trajectories can be trapped into a closed region of the phase space without converge into a limit cycle or settle down to a fixed point, and they could be attracted by a complex geometric object called strange attractor, which is a fractal set on which the motion is aperiodic and sensitive to very small changes in initial conditions. This sensitivity makes the motion unpredictable as *t* increases, giving rise to a chaotic dynamics [3].

Bifurcations

The qualitative features of the vector field of a biochemical dynamical system are strongly dependent on the set of parameters of its corresponding set of differential equations. As the value of one of these parameters changes, the qualitative features of the vector field undergo local variations around the steady points. This parameter-dependent change in the local topological structure of a vector field is known as bifurcation. They generally occur in a one-dimensional subspace, and the rest of the dimensions of the phase space are affected as

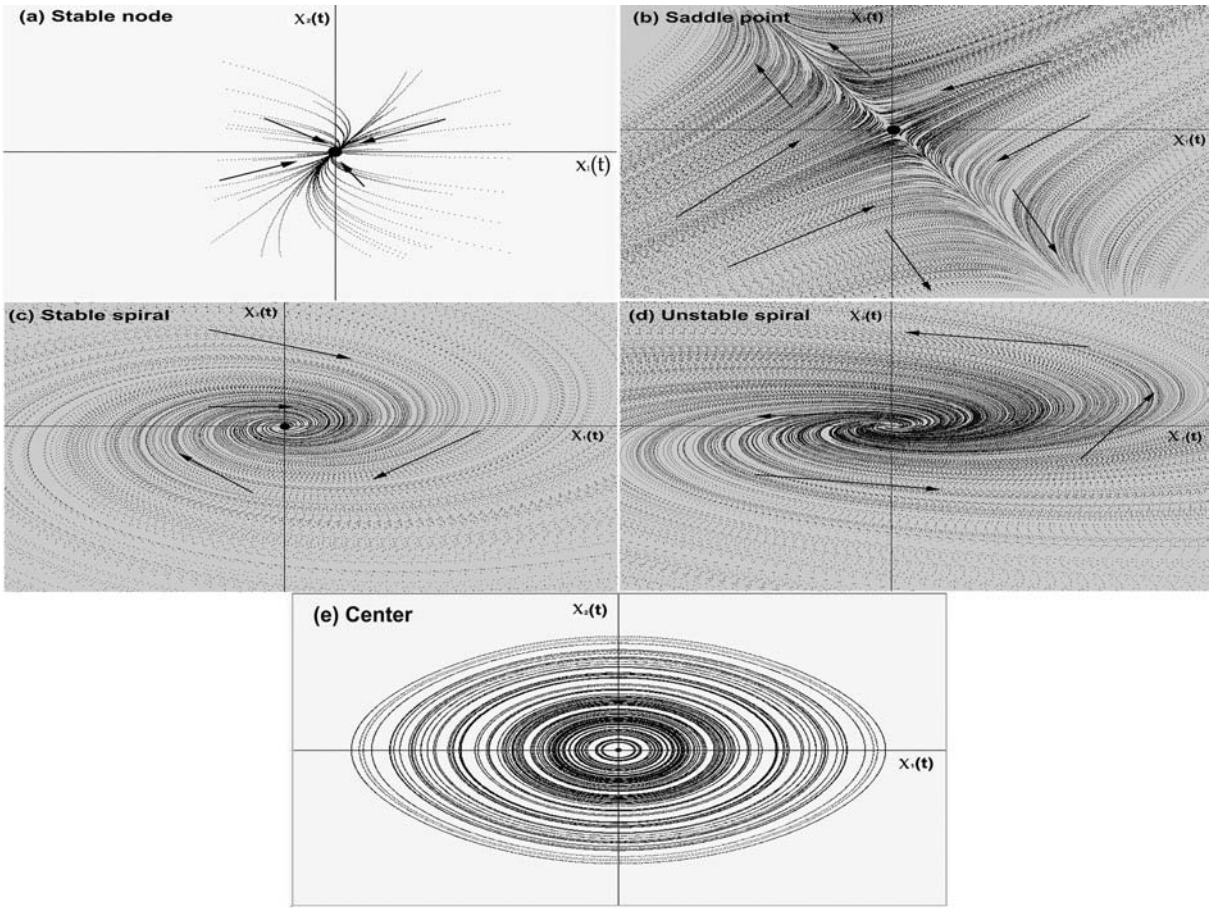

Figure A2. (a) There is a stable node or attractor in the phase space when both eigenvalues λ_1 and λ_2 are real and negative (when both eigenvalues are positive, the steady point is a unstable node or repulsor); (b) There is a saddle point in the phase space when both eigenvalues λ_1 and λ_2 are real, but one of them is positive and the other is negative. The stable manifold is spanned by the eigenvector associated to the negative eigenvalue. The unstable manifold is spanned by stable the eigenvector associated to the positive eigenvalue. (c) There is a stable spiral in the phase space when both eigenvalues λ_1 and λ_2 are complex conjugated with negative real part. (d) On the contrary, if both eigenvalues λ_1 and λ_2 are complex conjugated with positive real part the spiral is unstable. (e) When λ_1 and λ_2 are pure imaginary the steady point is a center surrounded by a series of stable closed orbits. All figures show the flow of the dynamical system in the phase space spanned by the basis conformed by the variables $x_1(t)$ and $x_2(t)$. The black point represents the steady point of the dynamical system, and the arrows mark out the direction of the flow of the vector field.

consequence of the flow that can be attracted or repelled from this subspace [3, 4]. Taking into consideration the imaginary plane, we can roughly classify bifurcations into two cases: 1) the eigenvalues of the Jacobian matrix are both real and bifurcations occur along the real axis as certain parameter α changes. This kind of bifurcation comprises the saddle-node bifurcation; the transcritical bifurcation, and the subcritical and supercritical pitchfork bifurcation. 2) The eigenvalues of the Jacobian matrix are complex conjugated. Bifurcations occur crossing the imaginary axis as certain parameter α changes. This kind of bifurcation comprises the supercritical and subcritical Hopf bifurcation.

In the first case, a) the saddle-node bifurcation causes local variations in the vector field around two points: a saddle and a node, as a bifurcation parameter α changes. These points become closer as parameter α varies until they collide and

annihilate each other. This type of bifurcation has interesting applications in some models of biological processes that imply the presence of chemical switches; b) a transcritical bifurcation occurs when two steady points interchange their stability as the bifurcation parameter α varies. c) The normal form of an ordinary differential equation (ODE) that exhibits a subcritical pitchfork bifurcation is $\dot{x} = \alpha x + x^3$. When α <0 the steady point x = 0 is stable and there are two unstable points at $x = \pm\sqrt{-\alpha}$. When α > 0 the only real steady point x = 0 becomes unstable. The normal form of an ODE that exhibits a supercritical pitchfork bifurcation is $\dot{x} = \alpha x - x^3$. When α < 0 the only real steady point x = 0 is stable. For α > 0 there is an unstable steady point at x = 0 and to stable steady points at $x = \pm\sqrt{\alpha}$.

In the second case, the presence of a Hopf bifurcation leads the system to a limit cycle. As the bifurcation parameter α varies, when a certain critical value α_c is reached the supercritical Hopf bifurcation drives the transformation of a stable spiral into an unstable spiral that converges to a stable limit cycle (Figure A3). The case of a subcritical Hopf bifurcation is more complicated. A typical example is when an unstable limit cycle shrinks to cero amplitude as the bifurcation parameter α reaches its critical value α_c, at which the cycle engulfs the node rendering it unstable and making the system to jump to a distant attractor when $\alpha > \alpha_c$ [3, 4]. This new attractor could be a steady point, another limit cycle, infinity or a chaotic attractor (for higher dimensional systems).

Reaction-diffusion equations

Equation (3) represents the chemical dynamics of substances without a homogeneous spatial distribution in the blastula. The nonlinear chemical term, represented by the function $f_k\left(x_1(\mathbf{r},t), x_2(\mathbf{r},t), ..., x_k(\mathbf{r},t), ...x_s(\mathbf{r},t)\right)$, induces the instability of the system, while the diffusion term $D_k\nabla^2 x_k(\mathbf{r},t)$ represents the flow of the substance k from zones of high concentration to zones of low concentration. These two forces are able of producing spatial stationary patterns of chemical concentration of a substance in the system, as well as chemical waves and spatially located bursting of some reactive component of the system.

In the particular case of two diffusive components, like IP3 and Ca^{2+}, Equation (3) can

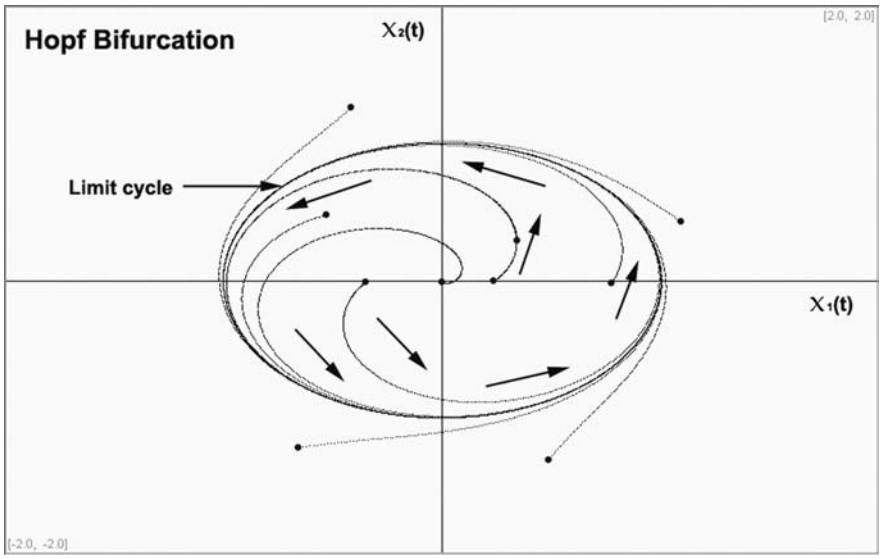

Figure A3. This kind of bifurcation transforms a stable spiral into an unstable spiral that converges to a stable limit cycle when the value of the bifurcation parameter α reaches some critical value α_c. The black points in the figure are different initial conditions of the dynamical system. The arrows mark out the direction of the flow of the vector field. The phase space is spanned by $x_1(t)$ and $x_2(t)$.

be written like a 1-dimensional, infinitely extended reaction-diffusion equation of the form:

$$\begin{aligned}\frac{\partial x_1(r,t)}{\partial t} &= f_1\big(x_1(r,t),x_2(r,t)\big) + D_1\frac{\partial^2 x_1(r,t)}{\partial r^2}\\ \frac{\partial x_2(r,t)}{\partial t} &= f_2\big(x_1(r,t),x_2(r,t)\big) + D_2\frac{\partial^2 x_2(r,t)}{\partial r^2}\end{aligned} \tag{8}$$

where $x_1(r,t) = IP3(r,t)$ and $x_2(r,t) = Ca^{2+}(r,t)$. This system has a spatially uniform steady-state:

$$x_1(r,t) = x_1^o \qquad x_2(r,t) = x_2^o \tag{9}$$

for which:

$$f_1\left(x_1^o, x_2^o\right) = 0 \qquad f_2\left(x_1^o, x_2^o\right) = 0 \tag{10}$$

perturbing this steady state:

$$\begin{aligned}x_1(r,t) &= x_1^o + \delta x_1(r,t)\\ x_2(r,t) &= x_2^o + \delta x_2(r,t)\end{aligned} \tag{11}$$

Substituting (11) en (8) and linearizing equation (8) we obtain:

$$\begin{aligned}\frac{\partial \delta x_1(r,t)}{\partial t} &= \left.\frac{\partial f_1(x_1,x_2)}{\partial x_1}\right|_{(x_1^o,x_2^o)}\delta x_1 + \left.\frac{\partial f_1(x_1,x_2)}{\partial x_2}\right|_{(x_1^o,x_2^o)}\delta x_2\\ &\quad + D_1\frac{\partial^2 \delta x_1(r,t)}{\partial r^2}\\ \frac{\partial \delta x_2(r,t)}{\partial t} &= \left.\frac{\partial f_2(x_1,x_2)}{\partial x_1}\right|_{(x_1^o,x_2^o)}\delta x_1 + \left.\frac{\partial f_2(x_1,x_2)}{\partial x_2}\right|_{(x_1^o,x_2^o)}\delta x_2\\ &\quad + D_2\frac{\partial^2 \delta x_2(r,t)}{\partial r^2}\end{aligned} \tag{12}$$

which in vectorial form can be written as:

$$\frac{\partial \delta \mathbf{x}}{\partial t} = \mathbf{J}\delta\mathbf{x} + \mathbf{D}\frac{\partial^2 \delta \mathbf{x}}{\partial r^2}$$

where:

$$\delta\mathbf{x} = \begin{bmatrix}\delta x_1\\ \delta x_2\end{bmatrix}$$

$$\mathbf{J} = \begin{bmatrix}\left.\frac{\partial f_1(x_1,x_2)}{\partial x_1}\right|_{(x_1^o,x_2^o)} & \left.\frac{\partial f_1(x_1,x_2)}{\partial x_2}\right|_{(x_1^o,x_2^o)}\\ \left.\frac{\partial f_2(x_1,x_2)}{\partial x_1}\right|_{(x_1^o,x_2^o)} & \left.\frac{\partial f_2(x_1,x_2)}{\partial x_2}\right|_{(x_1^o,x_2^o)}\end{bmatrix} = \begin{bmatrix}a_{11} & a_{12}\\ a_{21} & a_{22}\end{bmatrix}$$

$$\mathbf{D} = \begin{bmatrix}D_1 & 0\\ 0 & D_2\end{bmatrix} \tag{13}$$

From equation (13), the operator $\mathbf{H} = \mathbf{J} + \mathbf{D}\frac{\partial}{\partial r^2}$ leads to the linear problem:

$$\frac{\partial \delta \mathbf{x}}{\partial t} = \mathbf{H}\delta\mathbf{x} \tag{14}$$

The proposed solution of equation (14) can be built as:

$$\delta\mathbf{x}(r,t) = \sum_{k=1}^{\infty}\mathbf{C}\, e^{\lambda_k t}\cos(\omega_k r) \tag{15}$$

This equation shows that beyond diffusive instability, the nonlinearities can give rise to a complex spatio-temporal evolution of the system. As a matter of fact, the perturbations of the steady state can be formed by a great number of superimposed modes. The fastest growing modes (with the larger positive eigenvalues of the set $\{\lambda_k \mid k = 1, 2, 3,\ldots\}$) determine the overall system dynamics, however, the slowest ones also have a non negligible influence making practically impossible to analytically determine the final spatio-temporal pattern achieved by the system. An alternative approach to the analytical methods for determining the final spatio-temporal pattern of a reaction-diffusion system is the numerical simulation, which is broadly used in biology and, in particular, in the study of the calcium dynamics in single and coupled cells. In the particular case of the Xenopus embryo, this approach has been used to analyze the diffusive dynamics of Ca^{2+} in a ring of blastomeres at the MBT stage [5].

REFERENCES

1. Thieffry, D. and Romero, D. 1999, Biosystems, 50, 49.
2. Del Vecchio, D., Ninfa, A. J. and Sontag, E. D. 2008, Molecular Systems Biology, 4, 161.
3. Strogatz, S. 1994, Nonlinear Dynanics and Chaos. With applications to Physics, Biology, Chemistry, and Engineering, Perseus Books Publishing, LLC. Cambridge.
4. Edelstein-Kesher, L. 2005, Mathematical Models in Biology, Classics in Applied Mathematics, Siam, Philadelphia.
5. Díaz, J., Pastor, N. and Martínez-Mekler, G. 2005, Developmental Dynamics, 232, 301.